NIH Public Access
Author Manuscript
J Neurophysiol. Author manuscript; available in PMC 2008 June 20.

Published in final edited form as:
J Neurophysiol. 2007 March ; 97(3): 2239–2253.

Distinct synaptic dynamics of heterogeneous pacemaker neurons in an oscillatory network

Pascale Rabbah and **Farzan Nadim**
Department of Mathematical Sciences, New Jersey Institute of Technology, Newark, NJ 07102, Department of Biological Sciences, Rutgers University, Newark, NJ 07102

Abstract

Many rhythmically active networks involve heterogeneous populations of pacemaker neurons with potentially distinct synaptic outputs that can be differentially targeted by extrinsic inputs or neuromodulators, thereby increasing possible network output patterns. In order to understand the roles of heterogeneous pacemaker neurons, we characterized differences in synaptic output from the anterior burster (AB) and pyloric dilator (PD) neurons in the lobster pyloric network. These intrinsically distinct neurons are strongly electrically coupled, co-active and constitute the pyloric pacemaker ensemble. During pyloric oscillations, the pacemaker neurons produce compound inhibitory synaptic connections to the follower lateral pyloric (LP) and pyloric constrictor (PY) neurons, which fire out of phase with AB/PD and with different delay times. Using pharmacological blockers, we separated the synapses originating from the AB and PD neurons and investigated their temporal dynamics. These synapses exhibited distinct short-term dynamics, depending on the presynaptic neuron type, and had different relative contributions to the total synaptic output depending on waveform shape and cycle frequency. However, paired comparisons revealed that the amplitude or dynamics of synapses from either the AB or PD neuron did not depend on the postsynaptic neuron type, LP or PY. To address the functional implications of these findings, we examined the correlation between synaptic inputs from the pacemakers and the burst onset phase of the LP and PY neurons in the ongoing pyloric rhythm. These comparisons showed that the activity of the LP and PY neurons are influenced by the peak phase and amplitude of the synaptic inputs from the pacemaker neurons.

Keywords

central pattern generator; synaptic depression; motor system; stomatogastric; pyloric rhythm

INTRODUCTION

Many rhythmically active motor networks are driven by pacemaker neurons that act as core oscillators, synchronizing the activity of other network neurons into a coherent rhythmic pattern (Koshiya and Smith 1999; Marder and Bucher 2001; Smith et al. 1991; Tresch and Kiehn 2000; Wallen and Grillner 1987). In such pacemaker-driven pattern-generating networks, it is common that the pacemaker neurons use chemical synaptic inhibition to set the relative activity patterns of the remaining neurons (Eisen and Marder 1984; Tryba and Ritzmann 2000; Wolf 1992) and that the efficacy of these synapses can be altered by neuromodulators to reshape the network output (Harris-Warrick et al. 1998; Marder 1994). Moreover, heterogeneous populations of pacemaker neurons, as in the vertebrate respiratory

Corresponding author: Farzan Nadim, New Jersey Institute of Technology, Department of Mathematical Sciences, 323 Martin Luther King Blvd., Newark, NJ 07102, Phone: (973) 353-1541, Fax: (973) 353-5518 Email: farzan@njit.edu.

NIH-PA Author Manuscript
NIH-PA Author Manuscript
NIH-PA Author Manuscript

NIH-PA Author Manuscript

NIH-PA Author Manuscript

NIH-PA Author Manuscript

system, can be differentially targeted by neuromodulators thus increasing the number of possible network output patterns (Ramirez et al. 2004).

The rhythmically active pyloric central pattern generator of the spiny lobster, *Panulirus interruptus*, is driven by a pacemaker ensemble that consists of two intrinsically distinct neuron types, the anterior burster (AB) and two pyloric dilator (PD) neurons. The pacemaker neurons exhibit similar, but not identical, synaptic connections to all other follower neurons (Eisen and Marder 1982). During the ongoing pyloric rhythm (frequency 0.5 to 2 Hz), the AB and PD neurons are co-active due to their strong electrical coupling and hence produce a compound inhibitory chemical postsynaptic potential onto each of the follower neurons. In a recent study, we characterized the dynamics of the compound synapse from this pacemaker ensemble onto two classes of follower LP and PY neurons (Rabbah and Nadim 2005). The PY neurons always lag the LP neuron in their activity phase; thus, we examined the hypothesis that this phase lag is partially due to distinct synaptic inputs from the pacemaker ensemble. Surprisingly, our results showed that the total synaptic effect of the pacemaker ensemble on these two classes of follower neurons is identical.

Previous studies have reported that the AB and PD neurons evoke inhibitory postsynaptic potentials (IPSPs) in the follower neurons that differ in their neurotransmitter type, time course of release, reversal potential and ion selectivity (Eisen and Marder 1984, 1982; Rabbah et al. 2002). Furthermore, exogenous neuromodulators differentially affect the intrinsic and synaptic properties of these neuron types, subsequently altering their relative synaptic influence on follower neurons and thus on the pyloric oscillation pattern (Ayali and Harris-Warrick 1999; Harris-Warrick et al. 1998; Johnson and Harris-Warrick 1997). It is therefore important to characterize the individual synaptic outputs of the AB and PD neurons. In this study, we examined whether the synapses made by each of the pacemaker AB and PD neurons differ in their short-term plasticity, temporal dynamics and dependence on presynaptic waveform shapes. We first characterized the dynamics of the synapses from the AB and PD neurons as a combined unit and then individually after blocking each synapse. We activated the synapses using various injection stimuli applied to the voltage-clamped presynaptic neurons and recorded simultaneously from the follower LP and PY neurons. We also examined the correlations between parameters describing the individual pacemaker synapses and the activity phase of the follower neurons. Our results show that the synapses to each of the two classes of follower neurons exhibit distinct dynamics depending on the presynaptic pacemaker neuron type, AB or PD. These results suggest that neuromodulatory inputs can differentially accentuate one set of dynamics over the other, allowing for selective control of the activity phase of the postsynaptic targets and thus leading to different network outputs.

METHODS

Preparation and identification of the neurons

Adult male spiny lobsters (*P. interruptus*) were purchased from Don Tomlinson Fisheries (San Diego, CA) and maintained in artificial seawater tanks at 12–15°C until use. Prior to each dissection, the animals were anesthetized by cooling in ice for 30 minutes. The stomatogastric nervous system (STNS; including the STG, the esophageal and the commissural ganglia) was removed using standard methods (Harris-Warrick 1992; Selverston et al. 1976). The STG was desheathed to allow penetration of the cell bodies and superfused using normal saline at 18° C, pH 7.35, containing (in mM): 12.8 KCl, 479 NaCl, 13.7 $CaCl_2$, 10.0 $MgSO_4$, 3.9 $NaSO_4$, 11.2 Trizma base, and 5.1 Maleic acid.

For neuron impalement, glass microelectrodes were pulled using a Flaming-Brown micropipette puller (P87, Sutter Instruments, CA) and filled with 0.6 M K_2SO_4 + 0.02 M KCl (resistances of 8–13 MΩ). Identification of the neurons was accomplished by matching

NIH-PA Author Manuscript

NIH-PA Author Manuscript

NIH-PA Author Manuscript

intracellular action potential recordings to their corresponding extracellular recordings on motor nerves (Harris-Warrick 1992; Selverston et al. 1976). Intracellular recordings were made from the soma of the neurons using Axoclamp 2B amplifiers (Molecular Devices, Foster City, CA) and extracellular recordings were amplified using a Differential AC amplifier model 1700 (A-M Systems, Carlsborg, WA).

Isolation of synapses from the AB and PD neurons to the LP and PY neurons

During the normal ongoing pyloric rhythm, the AB and PD neurons oscillate in synchrony due to their strong electrical coupling and so the follower neurons experience a compound inhibitory postsynaptic potential from both the AB and PD neurons ($IPSP_{AB/PD}$). Voltage clamp stimulations of the two PD neurons in control saline are sufficient to elicit synaptic release from both AB and PD neurons (Rabbah and Nadim 2005). To characterize the synaptic dynamics of the AB and PD neurons separately, we stimulated the PD neurons while the preparation was superfused with 5 μM picrotoxin (PTX; Marder and Paupardin-Tritsch 1978). PTX blocks the glutamatergic synaptic release from the AB neuron and hence IPSPs recorded in the follower neurons were those elicited solely by the PD neurons ($IPSP_{PD}$). Because there are no known gap junctional blockers in the STG, in order to isolate the component of the chemical synapse that was elicited by the AB neuron ($IPSP_{AB}$), $IPSP_{PD}$ elicited in PTX conditions were digitally subtracted from $IPSP_{AB/PD}$ elicited in control conditions. In separate experiments, 1 mM tetraethylammonium (TEA) was used to block the cholinergic PD synapses (Marder and Eisen 1984). The results obtained when using TEA were not quantitatively significantly different from the results obtained when the PTX traces were subtracted from the control traces (data not shown; N = 5). The data reported in this study are from the subtracted traces only. Note that the low concentration of TEA used is not sufficient to significantly block potassium currents in these neurons (Graubard and Hartline 1991; Kloppenburg et al. 1999; Peck et al. 2001).

The pacemaker neurons are connected to the ventricular dilator VD neuron via a mixed chemical and electrical synapse. VD also forms inhibitory chemical connections to both the LP and PY neurons (Eisen and Marder 1982). As a precautionary measure to eliminate any possible contamination of the AB/PD induced IPSPs in the LP and PY neurons by the VD neuron, the VD neuron was photoinactivated in all experiments. The complete photoinactivation procedure is outlined in (Eisen and Marder 1984; Miller and Selverston 1979; Miller and Selverston 1982).

Comparison of $IPSP_{AB}$ and $IPSP_{PD}$ to the LP and PY neurons

The inhibitory synapses between the pacemaker neurons and the follower neurons use voltage-dependent (graded) release of neurotransmitter as the major form of transmission (Graubard 1978; Graubard et al. 1980; Johnson and Harris-Warrick 1990; Johnson et al. 1995; Maynard and Walton 1975). This form of synaptic release was isolated from the spike-mediated transmission by blocking the latter with *Panulirus* saline containing 10^{-7} M tetrodotoxin (TTX; Biotium, CA). Spontaneous rhythmic activity and modulatory inputs from anterior ganglia are also blocked by TTX (Raper 1979). The experiments were carried out in voltage clamp to better control the membrane potential of the presynaptic neurons. One PD neuron was voltage clamped with two electrodes to a holding membrane potential (V_{hold}) of −60 mV. The second PD neuron was impaled with one electrode. The current that was used to voltage clamp the first PD neuron was scaled up (using the specification of the amplifier) via a Brownlee Precision Amplifier (Santa Clara, CA) and injected into the second PD neuron to effectively voltage-clamp the second PD neuron to the same V_{hold} with only one electrode (see (Rabbah and Nadim 2005)). The LP and PY neurons were impaled with one electrode each and the graded IPSPs, elicited by the stimulation of the PD neurons, were recorded in current clamp (see schematic in Fig. 1B). Only paired recordings of the LP and PY were used in this study.

NIH-PA Author Manuscript

NIH-PA Author Manuscript

NIH-PA Author Manuscript

The properties of the synapses from the pacemaker neurons to the LP and PY neurons were studied using various injection protocols. Single square two-second depolarizing pulses (amplitudes ranging from 10 to 40 mV) were injected into the voltage clamped PD neurons to study the synapses in a static context. Trains of five square pulses (fixed 500 ms duration and 40 mV amplitude) with increasing interpulse intervals (IPIs; from 250 ms to 8000 ms) were used to study the extent of depression and recovery. Two realistic PD waveforms were built by recording voltage traces of the PD neurons in normal saline during slow (1358 ms) and fast (623 ms) pyloric cycle periods, averaging them over several cycles and low-pass filtering them at 10 Hz to remove action potentials (and thus isolate the graded transmission). The resulting two realistic waveforms were indexed by their duty cycles (DC; defined as the percentage of time, in each cycle, that the PD waveform was above its mean membrane potential). The waveform duty cycles were 17% and 46%, respectively. The two waveforms will be referred to by their DC values from now on. The waveforms were scaled to 40 mV (from through-to-peak) and played back periodically into the voltage clamped PD neurons. This allowed us to investigate the effects of varying presynaptic frequency (from 0.5–4 Hz) as well as the shape of presynaptic depolarizations (DC 17% and 46%) on the dynamics of the synaptic response in the LP and PY neurons. The same two waveforms were used in all experiments to allow for averaging of the data across preparations.

Whenever trains of pulses were used to activate the presynaptic neurons (square or realistic waveforms), the resulting IPSP maximal peak amplitudes were always measured from resting potential (V_{rest}) of the postsynaptic neuron as opposed to the respective baseline of each IPSP. This was done because at short inter-pulse intervals or periods, the IPSPs in each train did not have sufficient time to return to V_{rest} (see Figure 3 for example).

Cycle period and the LP and PY neuron burst times were measured using the PD neuron burst onset as reference (see Fig. 1A). The activity phase of the LP and PY neurons were calculated as the time difference (Δt) between the burst onset of that neuron and the onset of the PD neuron burst divided by cycle period.

Recording, Analysis and Statistics

An NI PCI-6070-E board (National Instruments, Austin, TX) was utilized for data acquisition and for current injection with the data acquisition software Scope developed in the LabWindows/CVI software environment (National Instruments, Austin, TX) on a Windows XP operating system. The acquired data were saved as individual binary files and were analyzed with the Readscope software. Scope and Readscope are software developed in the Nadim laboratory and are available for download at http://stg.rutgers.edu/software/index.htm). Digital subtraction of traces was done by custom-made programs written in LabWindows/CVI (National Instruments). Statistica (Statsoft, Tulsa, OK), SigmaStat (SPSS, San Rafael, CA) and Origin (OriginLab, Natick, MA) software packages were used for statistical and graphical analysis. Reported statistical significance indicated that the achieved significance level *P* was below the critical significance level $\alpha = 0.05$. When multiple comparisons were made, the alpha was corrected using the False Discovery Rate correction method (Curran-Everett 2000). In those cases, the value is given as B = corrected α value. All error bars shown and error values reported denote standard deviations.

RESULTS

The electrically coupled AB and two PD neurons compose the pacemaker unit of the pyloric circuit. These neurons oscillate in synchrony (Fig. 1A; top two traces; for simplicity, only one PD neuron is shown) and together, they drive the pyloric rhythmic activity. Each cycle of the tri-phasic pyloric rhythm is generated by a simultaneous burst in the pacemaker neurons, followed, with a short delay, by a burst in the LP neuron and then by a burst in the PY neurons

NIH-PA Author Manuscript

NIH-PA Author Manuscript

NIH-PA Author Manuscript

(Fig. 1A). The pacemaker AB and PD neurons are each connected to the follower LP and PY neurons via chemical inhibitory synapses (Fig. 1B) and so during normal ongoing rhythm, the AB and PD neurons produce a compound postsynaptic potential onto the LP and PY neurons.

In a recent publication (Rabbah and Nadim 2005), we compared the dynamics of the synapses between the pacemaker AB and PD neurons as a unit ($IPSP_{AB/PD}$) to the follower LP and PY neurons. Here, we examine instead the dynamics of the synaptic inputs the LP and PY neurons receive from the individual pacemaker AB ($IPSP_{AB}$) and PD ($IPSP_{PD}$) neurons. This analysis was done in three parts: First, we examine whether the intrinsically distinct AB and PD neurons exhibit distinct synaptic dynamics. Thus, we start by characterizing various parameters of $IPSP_{AB}$ and $IPSP_{PD}$ onto the LP and PY neurons using paired LP and PY recordings and various injection stimuli into the pacemaker neurons. Second, we examine whether the synapses originating from the same presynaptic neuron (AB or PD) onto two different classes of target neurons (LP and PY) exhibit distinct dynamics. Third, we ask whether these synaptic parameters correlate with and thus help determine the activity phases of the follower LP and PY neurons in the normal ongoing pyloric activity.

Comparison of the dynamics of $IPSP_{AB}$ and $IPSP_{PD}$ to the LP and PY neurons

To measure synaptic strength, we activated the pacemaker synapses using single two-second presynaptic square pulses of various amplitudes (Fig. 2). Figure 2A shows the synaptic response in the LP neuron when the PD neurons were stepped from − 60 mV to − 20 mV (top trace). The red trace represents the IPSPs elicited in the LP neuron in control (TTX) saline. This IPSP consists of the AB and PD components ($IPSP_{AB/PD}$). In the presence of PTX, the AB glutamatergic release is blocked and hence the LP neuron experiences synaptic release from the PD neurons only ($IPSP_{PD}$; blue trace). The AB component ($IPSP_{AB}$; black trace) was then approximated by digitally subtracting the PTX trace from the control trace (see Methods). All three IPSPs showed a large early peak (Fig. 2A; dotted arrows) that decayed to a sustained value (Fig. 2A; dashed arrows) during the stimulation period. The peak component of $IPSP_{AB}$ decayed faster than $IPSP_{AB/PD}$ or $IPSP_{PD}$.

At first glance, one may predict that since $IPSP_{PD}$ recorded in PTX was almost as large in amplitude as $IPSP_{AB/PD}$ recorded in control, the subtraction of the two traces would yield a much smaller $IPSP_{AB}$. However, Figure 2B shows that the delay from presynaptic onset to the onset of the postsynaptic response was different for $IPSP_{AB}$ and $IPSP_{PD}$. The AB to LP synapse was activated almost instantaneously upon presynaptic depolarization while the PD to LP synapse was activated with a ~60 ms delay (Fig. 2B; double headed arrow). Thus, $IPSP_{PD}$ reached its maximal peak later in time. Interestingly, once $IPSP_{PD}$ was activated, its rise time was similar to $IPSP_{AB}$, resulting in essentially no inflection on the rise of $IPSP_{AB/PD}$.

The maximal peak amplitudes of the IPSPs (measure of synaptic strength) elicited in response to all presynaptic depolarization amplitudes (V_{pre} from − 60 mV to − 50, − 40, − 30, − 20 mV) were normalized to the amplitude of $IPSP_{AB/PD}$ recorded in response to a step to 20 mV in control conditions. The resulting normalized I/O relationship is shown in Figure 2C. Note that ΔV_{LP} (and ΔV_{PY}) values are plotted as negative in this and subsequent figures in order to indicate the inhibitory nature of the synapse from the pacemaker neurons onto the LP (and PY) neuron. The IPSP amplitudes elicited in the LP neuron increased with increasing presynaptic potentials as expected from a graded synapse. Interestingly, in response to depolarization steps that shifted the membrane potentials of the presynaptic neurons relatively little (V_{pre} = − 50 and − 40 mV), we observed that the amplitudes of $IPSP_{AB/PD}$ were mostly due to the AB neuron (compare red and black traces). In those presynaptic voltage ranges, $IPSP_{PD}$ (blue trace) was significantly smaller in amplitude than $IPSP_{AB/PD}$ (two-way ANOVA, $p < 0.05$; $B = 1.67 \times 10^{-2}$; $N = 6$). With larger PD neuron depolarizations (V_{pre} to − 30 and − 20 mV), the chemical transmission from the PD neurons increased. In those voltage ranges, both $IPSP_{PD}$ and

NIH-PA Author Manuscript

NIH-PA Author Manuscript

NIH-PA Author Manuscript

$IPSP_{AB}$ were significantly smaller than $IPSP_{AB/PD}$ (two-way ANOVA, $p < 0.05$; $B = 1.67 \times 10^{-2}$; $N = 6$) and not significantly different from each other, indicating that both AB and PD neurons were contributing to the compound synapse.

Blocking the AB to LP direct synapse in PTX removed the AB short time to peak component, revealing a slower PD component (see Figs. 2A and B). To examine the time course of synaptic transmission, the time to peak of the IPSPs was quantified by calculating the Δt between the presynaptic pulse onset and the postsynaptic maximal peak hyperpolarization (Fig. 2D; inset). As the magnitude of presynaptic depolarization increased (V_{pre} values from − 60 mV to − 50, − 40, − 30, − 20 mV), the maximal postsynaptic responses in the LP neuron peaked earlier in time, independent of the identity of the presynaptic neuron (AB or PD) (Fig. 2D). However, the latency of the maximal peak hyperpolarization of $IPSP_{PD}$ onto LP was greater than that of $IPSP_{AB}$ (two-way ANOVA post-hoc Tukey analysis, $p \leq 0.048$ for V_{pre} to − 50, − 40 and − 30 mV; $N = 6$). Normalizing the Δt of the $IPSP_{PD}$ and $IPSP_{AB}$ to their respective Δt at the most depolarized presynaptic potential showed that the peak of the synapse from the PD neurons reached its maximal value 320% earlier as V_{pre} increased and 242% earlier for the synapse from the AB neuron (data not shown; one way ANOVA, $p \leq 0.040$ for both; $N = 6$).

The synaptic responses ($IPSP_{AB/PD}$, $IPSP_{PD}$ and $IPSP_{AB}$) recorded in the PY neuron during single square pulse stimulation of the PD neurons were not significantly different in strength and time course compared to those elicited in the LP neuron. Moreover, the normalized I/O curve of the IPSPs in the PY neuron (Fig. 2E) showed a similar trend to that observed in the LP neuron (Fig. 2C). Specifically, the compound $IPSP_{AB/PD}$ consisted mainly of the AB component at $V_{pre} = -50$ and − 40 mV and of both the AB and PD components at more depolarized presynaptic voltages. Plotting Δt_{PY} vs. V_{pre} showed that $IPSP_{PD}$ reached its maximal peak value significantly later at all presynaptic voltage values compared to $IPSP_{AB}$ (Fig. 2F; two-way ANOVA, post-hoc Tukey analysis, $p \leq 0.049$ for all V_{pre} values; $N = 6$).

To characterize the parameters of the short-term dynamics of the synapses (extent of depression and time course of recovery) from the pacemaker neurons to the LP and PY neurons, we used a train of square pulses of fixed duration and different inter-pulse intervals (IPIs: 250–8000 ms; Fig. 3). Figure 3A is an example showing the voltage traces of the LP neuron in response to a train of pulses with 500 ms IPI into the PD neurons. The synapses from $IPSP_{AB/PD}$ (red trace) as well as from the individual AB (black trace) and PD (blue trace) components showed short-term depression: the 2^{nd} and subsequent presynaptic depolarization pulses elicited IPSPs (Fig. 3A; vertical arrow) that were smaller in amplitude than those elicited by the 1^{st} pulse (Fig. 3A; horizontal arrow). Note that the amplitude of each IPSP was measured from the resting potential of the postsynaptic neuron (see Methods).

The extent of synaptic depression was quantified as the ratio of the final (5^{th}) IPSP peak amplitude to the first plotted vs. IPI (Mamiya et al. 2003; Rabbah and Nadim 2005) (Fig. 3B). At the shortest IPI, $IPSP_{PD}$ and $IPSP_{AB}$ exhibited the greatest depression and as the duration of the IPI increased, the magnitude of depression decreased (ratio of 1 indicates maximum recovery from depression). Even though $IPSP_{PD}$ tended to show more depression compared to $IPSP_{AB}$, statistically, their extent of depression (for IPSPs recorded in the LP neuron) was not significantly different from each other (two-way ANOVA, $p > 0.05$; $N = 6$). This trend was slightly more prominent in the responses recorded in the PY neuron (Fig. 3C; two-way ANOVA post-hoc Tukey analysis, $p < 0.001$ for IPI 250 ms; $N = 6$). However, for all IPIs tested, the extent of depression of the synaptic responses ($IPSP_{AB/PD}$, $IPSP_{PD}$ and $IPSP_{AB}$) recorded in the PY neuron were not significantly different compared to those elicited in the LP neuron (two-way ANOVA, $p > 0.05$; $N = 6$).

NIH-PA Author Manuscript

NIH-PA Author Manuscript

NIH-PA Author Manuscript

To fully characterize the parameters of short-term synaptic dynamics, we measured the time constant of recovery from depression by looking at the relationship between recovery and IPI. In each experiment, we graphed the ratio of the 5th peak/1st peak vs. IPI and fit it with a first order exponential decay curve with the equation $(1 - D_{max})\, e^{-IPI/\tau < sub > rec </sub >}$ (see Fig. 4E for example; also (Mamiya et al. 2003)). D_{max} is the maximum amount of depression of a synapse as IPI tends to zero and τ_{rec} is the time constant of recovery. Average τ_{rec} values for the synaptic depression in the LP neuron showed that $IPSP_{PD}$ (τ_{rec} = 311 ± 28.910 ms) tended to recover faster than $IPSP_{AB}$ (τ_{rec} = 478 ± 103.501 ms), although this difference was not statistically significant (paired t-test, p = 0.192; N = 6; data not shown). Similarly, $IPSP_{PD}$ to the PY neuron tended to recover from depression faster than $IPSP_{AB}$ but not significantly (τ_{rec} = 491 ± 110.692 ms and τ_{rec} = 576 ± 96.132 ms, respectively; data not shown). The time constant of recovery values for all IPSPs ($IPSP_{AB/PD}$, $IPSP_{PD}$ and $IPSP_{AB}$) recorded in the PY neuron were not significantly different compared to those recorded in the LP neuron (two-way ANOVA, p > 0.05; N = 6).

In the experiments described to this point, we used the conventional square pulse method (Johnson et al. 1995; Manor et al. 1997; Rabbah and Nadim 2005) to characterize various properties of the synapses from the pacemaker neurons onto the LP and PY neurons. However, it has been shown that square pulses do not fully capture the temporal dynamics of graded synapses (Manor et al. 1997; Olsen and Calabrese 1996). Graded synapses are sensitive to the shape of the presynaptic depolarizations and their frequency (Mamiya and Nadim 2004; Manor et al. 1997; Olsen and Calabrese 1996; Simmons 2002). Therefore, we voltage clamped the presynaptic PD neurons using two different realistic waveforms, pre-recorded during fast (623 ms) and slow (1358 ms) pyloric cycle periods (see Methods; also Rabbah and Nadim 2005). We indexed the change in waveform shape by the waveform duty cycle (DC) and chose two representative duty cycles 46% (Fig. 4A, top panel) and 17% (Fig. 4A, bottom panel) to stimulate the presynaptic neurons.

The realistic waveforms were applied into the two voltage clamped PD neurons from a baseline of −60 mV with a fixed 40 mV (trough to peak) amplitude and with cycle periods 250 to 2000 ms (frequency 4 to 0.5 Hz). Figure 4B shows an example of $IPSP_{AB/PD}$ (red traces), $IPSP_{PD}$ (blue traces), and $IPSP_{AB}$ (black traces) elicited in the LP neuron in response to a train of waveform stimulations corresponding to the duty cycle 46% (top traces) and 17% (bottom traces) and cycle period of 500 ms. As with trains of voltage pulses, all IPSPs showed short-term depression and recovered from depression as the cycle period was increased (Figs. 4C and 4D). Also, similar to trains of voltage pulses, the extents of depression of $IPSP_{PD}$ and $IPSP_{AB}$ in response to DC 46% (Fig. 4C) were statistically similar (two-way ANOVA p = 0.836; N = 6). Interestingly however, in response to DC 17%, $IPSP_{AB}$ exhibited significantly less depression compared to $IPSP_{PD}$ at the shortest IPIs tested (Fig. 4D; two-way ANOVA post-hoc Tukey analysis, p≤0.041 for periods 250, 500 and 1000 ms; N = 6).

We measured the time constant of recovery τ_{rec} of the IPSPs in response to the two realistic waveforms as previously described for Fig. 3 (see also Fig. 4E). Figure 4F shows that, in response to DC 46%, the PD component tended to recover from depression faster than the AB component but this tendency was not statistically significant (τ_{rec} = 390 ± 46.303 and 536 ± 98 ms, respectively; student's t-test, p = 0.198; N = 6). This trend was similar to the trend seen with the square pulse protocol. Interestingly however, when DC 17% was used, the trend of recovery from depression was reversed: The IPSP that the LP neuron received from the PD neuron recovered significantly slower from depression than the IPSP from the AB neuron (τ_{rec} = 510 ± 76.903 and 344 ± 34 ms, respectively; student's t-test, p = 0.029; N = 6).

We also activated the synapse between the pacemaker neurons and the PY neuron with the two presynaptic realistic waveforms in control and PTX conditions. Figure 5A shows an example

NIH-PA Author Manuscript

NIH-PA Author Manuscript

NIH-PA Author Manuscript

of $IPSP_{AB/PD}$ (red traces; control), $IPSP_{PD}$ (blue traces; PTX), and $IPSP_{AB}$ (black traces) recorded in the PY neuron in response to a train of waveform stimulations corresponding to DC 46% (top traces) and 17% (bottom traces) and cycle period of 500 ms. All IPSPs showed short-term depression as the cycle period was increased (Figs. 5B and 5C). Unlike what was seen in the LP neuron, in response to both PD realistic waveforms, $IPSP_{AB}$ exhibited significantly less depression compared to $IPSP_{PD}$ (two-way ANOVA, post-hoc Tukey analysis, $p \leq 0.042$ for periods 250, 500, 1000, 1500 and 2000 ms; N = 6). However, comparison of the extents of depression in the LP vs. PY neurons due to $IPSP_{PD}$ and $IPSP_{AB}$ were not significantly different from each other (two-way ANOVA, $p > 0.05$; N = 6).

Measurement of the time constant of recovery τ_{rec} of the IPSPs in response to the two realistic waveforms showed similar trends to the LP neuron (compare Fig. 4F with Fig. 5F). In response to activating the presynaptic neurons with DC 46%, the PD to PY component tended to recover from depression faster than the AB component (τ_{rec} = 410 ± 48.304 and 580 ± 136.703 ms, respectively; student's t-test, p = 0.142; N = 6). Moreover, with DC 17%, $IPSP_{PD}$ tended to recover slower from depression than the synapse from the AB neuron (τ_{rec} = 599 ± 110 and 364 ± 80.902 ms, respectively; student's t-test, p = 0.141; N = 6). Neither of these trends was statistically significant. Also, the τ_{rec} values for the LP vs. PY neurons due to $IPSP_{PD}$ and $IPSP_{AB}$ were not significantly different from each other (two-way ANOVA, $p > 0.05$; N = 6).

The maximal peak amplitude of the IPSP in the LP neuron elicited by either AB or PD components appeared sensitive to the slope of the rising phase of the presynaptic depolarizations (Fig. 6). We focus on the IPSPs in response to the 5^{th} waveform (see Fig. 5A) because it carries information about the dynamics of the "stationary" synapses after transient changes are over. Figure 6A presents a comparison of the amplitudes of the 5^{th} IPSPs elicited with DC 46% (left panel) with those elicited with DC 17% (right panel) corresponding to cycle period 500 ms. We observed that, in response to DC 46%, $IPSP_{AB}$ was smaller in amplitude than $IPSP_{PD}$ (Fig. 6A, left panel, compare black and blue traces). Similar to square pulses, we measure the amplitude of each IPSP from V_{rest}. However, in response to DC 17%, $IPSP_{AB}$ and $IPSP_{PD}$ appeared equal in amplitude (Fig. 6A, right panel, compare black and blue traces). To illustrate the relative contribution of the AB and PD components to the total synaptic transmission onto the LP neuron (Fig. 6A, red traces), we normalized the steady-state amplitudes of $IPSP_{PD}$ and $IPSP_{AB}$ to the steady-state amplitude of $IPSP_{AB/PD}$ at frequency 0.67 Hz and plotted the values as a function of presynaptic frequency (Figs. 6B for DC 46% and 6C for DC 17%). The results of the data presented in these two panels are two-fold. First, $IPSP_{AB}$ showed no dependence on presynaptic frequency irrespective of the presynaptic waveform used (one-way ANOVA, p = 0.151 for DC 46% and p = 0.438 for DC 17%; N = 6) indicating that the AB synapse is activated to the same extent for all presynaptic frequencies and duty cycles tested. In contrast, the steady-state amplitudes of $IPSP_{PD}$ significantly decreased as the frequency was increased (one way ANOVA, $p < 0.001$ for both DC 46% and 17%; N = 6). Second, the relative contribution of the PD neurons compared to the AB neuron was dependent on the shape of the presynaptic waveform: When the presynaptic waveform with DC 46% was used, $IPSP_{PD}$ recorded in the LP neuron at all frequencies (except 4 Hz) was significantly larger in amplitude than $IPSP_{AB}$ (Fig. 6B; two-way ANOVA post-hoc Tukey analysis, $p \leq 0.004$ for frequency 0.5, 0.67, 1 and 2 Hz; N = 6). In contrast, when DC 17% was used, $IPSP_{PD}$ and $IPSP_{AB}$ were recruited to similar levels for most frequencies tested (Fig. 6C; two-way ANOVA post-hoc Tukey analysis, $p \leq 0.026$ for frequency 0.5 and 0.67 Hz only; N = 6). These results suggest that, at low frequencies, the synapse from the pacemaker unit onto the LP neuron is dictated mostly by the PD neurons for both presynaptic duty cycles tested. As the frequency of the presynaptic depolarization is increased, the PD neuron contribution decreases and approaches the (unchanging) AB neuron contribution but to different extents depending on the duty cycle of the presynaptic waveform.

NIH-PA Author Manuscript

NIH-PA Author Manuscript

NIH-PA Author Manuscript

We repeated all of the above measurements for the PY neuron (Fig. 7). Figure 7A shows a comparison of the amplitudes of the steady-state IPSPs elicited in the PY neuron with DC 46% (left panel) with those elicited with DC 17% (right panel) corresponding to cycle period of 500 ms. Similar to the results obtained in the LP neuron at that cycle period, (steady-state) $IPSP_{AB}$ elicited due to DC 46% was smaller in amplitude than $IPSP_{PD}$ (Fig. 7A left panel) while $IPSP_{AB}$ in response to DC 17% was equal in amplitudes to $IPSP_{PD}$ (Fig. 7A; right panel). When the steady-state amplitudes of $IPSP_{PD}$ and $IPSP_{AB}$ were normalized to the steady-state amplitude of $IPSP_{AB/PD}$ at frequency 0.67 Hz and plotted as a function of presynaptic frequency (Figs. 7B for DC 46% and 7C for DC 17%), we saw that the relative amplitudes of $IPSP_{PD}$ and $IPSP_{AB}$ were significantly different in response to DC 46% at most presynaptic frequencies tested (Fig. 7B; two-way ANOVA post-hoc Tukey analysis, $p \leq 0.048$ for frequency 0.5, 0.67, 1 and 2 Hz; N = 6) but statistically similar in response to DC 17% at all frequencies (Fig. 7C; two-way ANOVA, $p > 0.05$; N = 6). $IPSP_{AB}$ showed no dependence on presynaptic frequency irrespective of which presynaptic waveform was used (one-way ANOVA, $p > 0.05$; N = 6) while $IPSP_{PD}$ significantly decreased as the frequency was increased (one way ANOVA, $p = 0.025$ for DC 46% and $p = .007$ for DC 17%; N = 6). These results indicate that, dependent on the duty-cycle of the presynaptic depolarization, $IPSP_{PD}$ contribution to the pacemaker synapse onto the PY neuron is either larger than the $IPSP_{AB}$ (DC 46%) or relatively equal to $IPSP_{AB}$ (DC 17%). The relative amplitudes of $IPSP_{PD}$ and $IPSP_{AB}$ in the LP vs. the PY neurons were not significantly different from each other (two-way ANOVA $p > 0.05$; N = 6)

The time-to-peak of the IPSPs provides information about the time course of synaptic transmission. Thus, we compared the changes in the peak time of the IPSPs in response to the stationary (i.e. 5^{th}) presynaptic realistic waveform stimulations for all frequencies tested (Fig. 8 for LP and Fig. 9 for PY). Figure 8A (and Fig. 9A for PY) shows a comparison of the time course of synaptic transmission for the stationary $IPSP_{PD}$ and $IPSP_{AB}$ in response to DC 46% (top panel) and DC 17% (bottom panel) corresponding to the frequency of 2 Hz. In response to both realistic waveforms in the PD neurons, the onset of the IPSP from the PD neurons was delayed compared to the onset of the IPSP from the AB neuron (Fig. 8A for LP and Fig. 9A for PY; double-headed arrows). This delay in the onset of the synaptic response affected the time the response needed to reach its maximal hyperpolarization peak (and decay): For DC 46%, the PD to LP (and PY) transmission reached its maximum peak at the end of the waveform depolarization while the AB to LP (and PY) maximum synaptic peak was perfectly aligned with the presynaptic depolarization peak (Fig. 8A for LP and Fig. 9A for PY, top panels, compare blue and black open circles). For DC 17%, maximum peak $IPSP_{PD}$ occurred after the depolarization was over (Fig. 8A for LP and Fig. 9A for PY, bottom panels, compare black and blue open circles). Similar to the results obtained with the square pulse stimulation of the presynaptic neurons, these results suggest that the PD synapses exhibit delayed (compared to the AB synapse) inhibitory actions in the LP and PY neurons.

We examined the frequency-dependent effect of this delay in synaptic transmission to the peak phase of the IPSPs in the LP and PY neurons. Phase describes the normalized (by period) time of the IPSP peak in the postsynaptic neuron relative to the presynaptic oscillations. We calculated phase as $\Delta t/period_{applied}$ where Δt was measured from the most depolarized peak of the presynaptic waveform to the maximum hyperpolarized peak of the IPSP (see Fig. 8B inset for example). The values were then plotted versus frequency for DC 46% (Fig. 8B for LP and Fig. 9B for PY) and DC 17% (Fig. 8C for LP and Fig. 9C for PY). Note that negative values of peak phase indicate that the IPSP actually reached its maximal hyperpolarized peak before the presynaptic waveform reached its maximal depolarized value. The LP (and PY) IPSP peak phase was significantly delayed due to the synapse from the PD neuron in comparison to the synapse from the AB neuron, independent of presynaptic waveform type (two-way ANOVA, LP: $p = 0.001$ for DC 46% and $p = 0.015$ for DC 17%, PY: $p = 0.003$ for DC 46% and DC 17%; N = 6). Moreover, we found that the peak phase of the IPSPs due to

NIH-PA Author Manuscript

NIH-PA Author Manuscript

NIH-PA Author Manuscript

the individual AB and PD components in response to both presynaptic realistic waveforms showed a dependence on presynaptic frequency in both the LP and PY neurons (one-way ANOVA, $p < 0.001$; $N = 6$). As frequency increased, the postsynaptic IPSP peaked later in phase. There was also a dependence on the waveform duty cycle: activating the presynaptic neurons with DC 46% and frequency 0.5 to 1 Hz acted to significantly advance the peak phase of both $IPSP_{PD}$ and $IPSP_{AB}$ in the LP and PY neurons (DC 46% vs. DC 17%: two-way ANOVA, post-hoc Tukey analysis, $p < 0.05$ for frequency 0.5, 0.67 and 1 Hz; $N = 6$). The peak phases of $IPSP_{PD}$ and $IPSP_{AB}$ in the LP vs. PY neurons for both realistic waveforms were statistically similar to each other (two-way ANOVA, $p > 0.05$; $N = 6$).

Correlation between the dynamics of $IPSP_{AB}$ and $IPSP_{PD}$ on the phase onset of the LP and PY neurons

Thus far, we have shown that the synaptic dynamics of the pacemaker AB and PD neurons exhibit distinct dynamics dependent on the frequency and shape of the presynaptic depolarizations. Specifically, the synaptic transmission from the PD neurons is a relatively slow process that serves to delay the peak of the hyperpolarization in the postsynaptic LP and PY neurons (and thus their IPSP peak phase) at all presynaptic frequencies. The opposite is true for the synaptic transmission from the AB neuron. Moreover, the relative contributions of the AB and PD neurons to the total synaptic output onto the LP and PY neurons change as a function of presynaptic depolarization, frequency and duty cycle of the injected stimuli. We have also shown that the dynamics of the synapses originating from either presynaptic pacemaker neuron (AB or PD) to the LP neuron vs. the PY neurons are not distinct from each other. We now investigate the functional importance of synaptic dynamics for the burst phase of postsynaptic neurons in a network driven by strongly electrically coupled pacemaker neurons that evoke distinct synaptic dynamics onto the same subset of neurons.

We begin by examining the relationship between the amplitudes of $IPSP_{PD}$ and $IPSP_{AB}$ and the activity phase of the LP neuron during the ongoing rhythm. Figure 10A presents a correlation of the LP burst phase during the ongoing rhythm to the amplitudes of the steady-state IPSPs measured in the LP neuron when the PD neurons were activated with DC 46% (left panel) and DC 17% (right panel). The LP burst phase was calculated using the natural pyloric period and the PD neuron as a reference, before the application of TTX (see Methods). As representative, we chose the stationary amplitudes of the IPSPs at cycle period of 1 s (frequency 1 Hz). The correlations made using cycle period 0.5 s produced similar results (data not shown). Each point on the graph represents one preparation.

In response to DC 46%, the LP burst phase (during the normal ongoing rhythm) showed a strong positive correlation to the amplitudes of both the measured $IPSP_{PD}$ and $IPSP_{AB}$ (Fig. 10A left panel: for $IPSP_{PD}$: $y = 0.018x + 0.612$, $r = 0.752$, $p = 0.021$; for $IPSP_{AB}$: $y = 0.028x + 0.621$, $r = 0.894$, $p = 0.001$). This relationship existed regardless of the duty cycle of the PD realistic waveform used to measure the IPSP (Fig. 10A right panel: for $IPSP_{PD}$: $y = 0.016x + 0.612$, $r = 0.773$, $p = 0.014$; for $IPSP_{AB}$: $y = 0.025x + 0.603$, $r = 0.791$, $p = 0.011$). These strong correlations indicate that, as the strengths of the synapses increase, the phase of the postsynaptic LP neuron burst onset occurs earlier, irrespective of the identity of the presynaptic neuron or its duty cycle. This correlation is further supported by Fig. 10B which shows that the amplitude of the compound synapse $IPSP_{AB/PD}$ in response to DC 46% (open squares) and 17% (filled squares) was also strongly positively correlated to the LP burst phase in the natural rhythm (for DC 46%: $y = 0.012x + 0.604$, $r = 0.761$, $p = 0.021$; for DC 17%: $y = 0.013x + 0.621$, $r = 0.792$, $p = 0.012$).

The correlation between the strength of the IPSPs and the LP burst phase does not account for the distinct temporal dynamics of $IPSP_{PD}$ and $IPSP_{AB}$. Thus, we calculated the IPSP time-to-peak with respect to the presynaptic stimuli (see Fig. 8B inset as example), divided the values

NIH-PA Author Manuscript

NIH-PA Author Manuscript

NIH-PA Author Manuscript

by the applied period of 1 s ($P_{applied}$) and examined their correlation to the LP burst phase during the natural pyloric rhythm (Mamiya et al. 2003). The right and left panels of Fig. 10C are scatter plots of these results using DC 46% and 17%, respectively. Our results show that when the presynaptic stimulus has a duty cycle of 46% or 17%, the burst phase of the LP neuron is not correlated to the IPSP peak phase it receives from either the PD (blue stars) or AB (black stars) neuron. In addition, the peak phase of $IPSP_{AB/PD}$ was not correlated to the LP burst phase with either waveform (Fig. 10D).

In contrast to what was seen in the LP neuron, in response to either presynaptic waveform, the PY burst phase (during the normal ongoing rhythm) showed a weak negative correlation to the amplitudes of both $IPSP_{PD}$ and $IPSP_{AB}$; i.e, as the IPSP amplitudes increased, the PY phase was delayed (Fig. 11A, left panel for DC 46%: $IPSP_{PD}$: $y = -0.014x + 0.601$, r = −0.601, p = 0.251; $IPSP_{AB}$: $y = -0.01x + 0.651$, r = −0.450, p = 0.371; right panel for DC 17%: $IPSP_{PD}$: $y = -0.015x + 0.592$, r = −0.931, p = 0.021; $IPSP_{AB}$: $y = -0.015x + 0.612$, r = − 0.611, p = 0.111). In response to both waveforms, the amplitude of the compound synapse $IPSP_{AB/PD}$ was also weakly negatively correlated to the burst phase of the PY neuron (Fig. 11B; for DC 46%: $y = -0.01x + 0.592$, r = −0.791, p = 0.112; for DC 17%: $y = -0.015x + 0.572$, r = − 0.821, p = 0.081).

Correlation of the IPSP peak phases with respect to $P_{applied}$ to the PY burst phase during the natural pyloric rhythm are shown in Figures 11C and 11D. With DC 46% or 17%, the burst phase of the PY neuron tended to be very weakly negatively correlated to the IPSP peak phase it receives from the AB neuron only (Fig. 11C; for DC 46% $y = -0.51x + 0.589$; r = −0.687; p = 0.131; For DC 17%: $y = -1.42x + 0.616$; r = − 0.602; p = 0.205; N = 6). In addition, the peak phase of the compound synapse $IPSP_{AB/PD}$ was negatively correlated to the LP burst phase when the presynaptic neurons were activated with either duty cycles (Fig. 11D; for DC 46% $y = -0.502x + 0.649$; r = −0.731; p = 0.098; For DC 17%: $y = -6.04x + 0.841$; r = − 0.947; p = 0.004; N = 6).

DISCUSSION

In a pacemaker driven oscillatory network, the synaptic interactions between the pacemaker neurons and the follower neurons are of crucial importance. These synapses can play a role in setting the activity phase of the follower neurons and the frequency of the rhythmic output (Eisen and Marder 1984; Tryba and Ritzmann 2000; Wolf 1992). However, when neural networks employ a heterogeneous population of pacemaker neurons, a greater level of complexity is added to the effect of pacemaker synapses on the relative phase relationships of member neurons. In the lobster pyloric network, the AB and PD pacemaker neurons produce compound chemical synapses to the follower LP and PY neurons. The compound synapses from these pacemaker neurons to the LP and PY neurons are identical in strength and dynamics and thus do not play a role in determining the relative activity phase of these follower neurons (Rabbah and Nadim 2005). However, neuromodulatory inputs to the pyloric network can differentially affect the intrinsic and synaptic properties of the AB and PD neurons as well as the strength of the electrical coupling between them (Harris-Warrick et al. 1998; Johnson and Harris-Warrick 1997; Johnson et al. 1993). In this manner, neuromodulators can emphasize one type of pacemaker neurons (and their synaptic connections) over the other, thus leading to a different functional network output. It is thus important to investigate the dynamics of the synapses originating from the AB and PD neurons separately and not only as a compound synapse.

We report a detailed examination of the temporal dynamics of the AB and PD synapses. Our work builds on previous studies of Eisen and Marder who reported on the neurotransmitter content, reversal potential and ion selectivities of these two synapses, as well as their time

NIH-PA Author Manuscript

NIH-PA Author Manuscript

NIH-PA Author Manuscript

course of release (Eisen and Marder 1984, 1982; Marder and Eisen 1984). We investigated the temporal dynamics of the synapses from the AB and PD synapses separately, in the absence of network neuromodulation, and addressed the functional implications of these synaptic dynamics in predicting the time of activity of the follower neurons.

Synaptic efficacy depends on presynaptic waveform shape and frequency

Our results show that the relative contributions of $IPSP_{AB}$ and $IPSP_{PD}$ to the compound AB/PD synapse in the LP and PY neurons are dependent on the shape of presynaptic waveform and frequency. We activated the PD neurons with two distinct realistic waveforms, with short (DC 17%) and long (DC 46%) duty cycles at the same amplitude and frequency, and recorded the postsynaptic responses (Fig. 6 for LP and 7 for PY). For all frequencies tested except 4 Hz, in response to DC 46%, $IPSP_{PD}$ recorded in the LP and PY neurons was significantly larger than $IPSP_{AB}$. However, in response to DC 17%, $IPSP_{PD}$ to the LP neuron was significantly larger at low frequencies (0.5 and 0.67 Hz) only. Taken together, these results indicate that the strength of the AB/PD synapse to the LP and PY neurons can be dictated either mostly by the PD neurons (as in the case of DC 46%) or by both the AB and PD neurons (as in the case of DC 17%), in a manner dependent on cycle frequency. Changes in cycle frequency are commonly induced in the pyloric circuit by network neuromodulators (Marder and Thirumalai 2002). In this manner, depending on the state of the network (i.e. which neuromodulator is present), frequency (and duty cycle) can be altered, allowing either one or both of the pacemaker AB and PD neurons, and the temporal dynamics of their synaptic outputs, to be important determinants of network output.

Short-term depression of the synapses is dependent on the membrane potential oscillation waveform of the PD neurons

Short-term depression allows for the dynamic control of synaptic strength between network neurons as a function of cycle period (Manor et al. 2003; Nadim and Manor 2000). Our results indicate that the short-term depression of $IPSP_{AB}$ and $IPSP_{PD}$ in the LP and PY neurons depend on the membrane potential waveforms of pacemaker neurons. Specifically, in response to waveforms with the sharpest rise time (square pulses) and longest duty cycle (DC 46%) activated with cycle periods comparable to the range of periods of the pyloric rhythm *in vivo* (Rezer and Moulins 1983; Turrigiano and Heinzel 1992), the synapses from the AB and PD neurons to the LP neuron depressed and recovered from depression to the same extent. However, in response to DC 17%, $IPSP_{AB}$ depressed significantly less and recovered significantly faster. In the case of the PY neuron, the short-term dynamics observed for $IPSP_{AB}$ and $IPSP_{PD}$ were similar for the square pulses but different for both realistic waveforms used. These results indicate that the kinetics of depression and recovery of the pyloric synapses are tuned so that the synaptic transmission is sensitive to period and duty cycle in the range over which the pyloric network normally operates (Mamiya and Nadim 2004, 2005; Manor et al. 1997). For example, in response to perturbations that increase cycle period and decrease duty cycle of the pacemaker neurons, the amplitudes of the pacemaker synapses to the LP and PY neurons will exhibit less depression and hence grow stronger. Such perturbations, elicited by neuromodulatory or synaptic inputs, can potentially modify the influence of the pacemaker neurons on the activity patterns of the follower neurons merely by changing the pacemaker membrane potential waveforms.

Measured IPSP peak amplitude as a predictive measure of the burst phase of the follower neurons in the normal ongoing rhythm

We were interested in investigating whether the relative amplitudes of the AB and PD synapses onto the LP and PY neurons measured in TTX conditions serve as predictive measurements of the burst phase of the LP and PY neurons in the ongoing rhythm. We found that the amplitude

NIH-PA Author Manuscript

NIH-PA Author Manuscript

NIH-PA Author Manuscript

of the LP IPSP due to either the AB or PD neurons was strongly positively correlated to the LP burst phase in the ongoing rhythm; the larger the IPSP, the earlier the LP burst phase. This is consistent with activating a hyperpolarization-activated inward current I_h, a current that is very prominent in the LP neuron and is responsible for the advancement of its burst phase following hyperpolarization (Harris-Warrick et al. 1995a; 1995b; Tierney and Harris-Warrick 1992). In contrast to the findings in the LP neuron, but similar to the findings of Mamiya et. al. (2003), a larger IPSP in the PY neuron (evoked by either AB or PD) resulted in a negative correlation to the PY burst phase in the ongoing rhythm. In this case, the larger IPSP most likely serves to activate larger amounts of the fast transient potassium current $I_{A,}$ a subthreshold current involved in the post-inhibitory property of the pyloric neurons (Graubard and Hartline 1984; Harris-Warrick 1989; Tierney and Harris-Warrick 1992). Hyperpolarization removes inactivation from this current and, when activated, it can delay the burst onset of the postsynaptic neuron (Harris-Warrick et al. 1995a). A clear understanding of the functional effects of the pacemaker IPSPs on the activity phases of the follower LP and PY neurons, however, requires further experiments that also take into account the synaptic connectivity between the follower neurons (Mamiya et al. 2003; Mamiya and Nadim 2005).

Measured IPSP peak phase as a predictive measure of the burst phase of the follower neurons in the normal ongoing rhythm

Synaptic outputs from the PD neurons are relatively slow, producing delayed peaks in the postsynaptic potentials of the LP and PY neurons at all presynaptic frequencies. The opposite is true for synaptic transmission from the AB neuron. It is expected that a delayed IPSP peak phase produce a delayed burst in the postsynaptic neuron. However, when we examined the relationship between the IPSP peak phase at various presynaptic periods and the phase of the LP neuron in the ongoing rhythm, we found no correlation between the two (Fig. 5.10B). In contrast, when PY was the postsynaptic neuron, the burst phase tended to be (weakly) negatively correlated to the phase of $IPSP_{AB}$. This latter result is consistent with faster removal of inactivation of an outward current in the PY neuron. The PY neuron, and not the LP neuron, possesses large amounts of I_A (Baro et al. 2000;Graubard and Hartline 1984;Harris-Warrick 1989;Tierney and Harris-Warrick 1992). It is plausible that if the IPSP in the PY neuron peaks earlier, a larger outward current is produced upon rebound from inhibition, thus delaying the PY burst onset.

The absence of very strong correlations between the measured synaptic parameters and the burst phase of the follower LP and PY neurons in the ongoing rhythm is not completely unexpected. The pyloric neurons form a multitude of synaptic connections with each other, including mixed electrical and chemical synaptic connections between the LP neuron and PY neurons (Mamiya et al. 2003). Moreover, the pyloric neurons have a variety of nonlinear intrinsic ionic currents (Golowasch and Marder 1992; Johnson et al. 2003; Kloppenburg et al. 1999). Thus, in an ongoing rhythm, the activity patterns of the LP and PY neurons are probably determined, not only by inputs from the pacemaker neurons, but by a dynamic combination of their intrinsic properties and various parameters of all their synaptic inputs, including strength, rate of transmission, and extent of depression and recovery (Golowasch et al. 1992; Harris-Warrick et al. 1995a; Hartline and Gassie 1979; Mamiya et al. 2003).

Contribution of synaptic dynamics from the pacemaker neurons in determining the relative activity phase of the LP and PY neurons

We have previously reported that the dynamics of the synapses that the LP and PY neurons receive from the pacemaker ensemble are not different from each other (Rabbah and Nadim 2005). In this study, we found that the dynamics of the synapses originating from either presynaptic pacemaker neuron (AB or PD) onto the LP neuron vs. the PY neurons are not distinct from each other either. The possibility still exists, however, that neuromodulators can

NIH-PA Author Manuscript

NIH-PA Author Manuscript

NIH-PA Author Manuscript

alter short-term dynamics of the AB and PD synapses, thus breaking this homogeneity. Modulation of short-term depression has been previously reported for the LP to PD synapse in crab *Cancer borealis* by the neuromodulator proctolin. Proctolin induced a shift from depression to facilitation of the LP to PD synapse, dependent on the amplitude of presynaptic depolarizations (Atamturktur et al. 2004). In this manner, neuromodulators can affect the total synaptic output of the pacemaker neurons, thus allowing the AB and PD neurons to play a role in setting the relative activity phase of the LP and PY neurons.

Conclusion

We showed that, in a pacemaker driven oscillatory network, the neurons that comprise the pacemaker ensemble can exhibit distinct synaptic dynamics onto the same classes of follower neurons. This heterogeneity provides the neural network with a mechanism for differential control of the relative contribution of each class of pacemaker neuron and its efferent targets to the overall network output. The principles reported in this work are not unique to invertebrate systems, but may be important for the generation of oscillatory activity in vertebrates. For example, the rhythmic activity of the inspiratory phase of the mammalian respiratory network is generated by a heterogeneous population of pacemaker neurons (Thoby-Brisson and Ramirez 2001). As in the crustacean pyloric pacemakers, the expression patterns of the mammalian respiratory pacemaker neurons are dependent on the state of the network, allowing for various functional outputs (Pena et al. 2004; Ramirez et al. 2004). It is thus important to emphasize that in order to fully understand the role of pacemaker neurons in shaping network output patterns we must not only examine their intrinsic and synaptic properties but also how these components can be modified by neuromodulatory inputs.

Acknowledgements

This work was supported by NIH MH-60605 (FN).

References

Atamturktur S, Manor Y, Nadim F. Proctolin enables a shift in synaptic dynamics from depression to facilitation due to the presyaptic waveform amplitude in a rhythmic network. Annual Meeting of the Society for Neurosience 2004:657.618.

Ayali A, Harris-Warrick RM. Monoamine control of the pacemaker kernel and cycle frequency in the lobster pyloric network. J Neurosci 1999;19:6712–6722. [PubMed: 10415000]

Baro DJ, Ayali A, French L, Scholz NL, Labenia J, Lanning CC, Graubard K, Harris-Warrick RM. Molecular underpinnings of motor pattern generation: differential targeting of shal and shaker in the pyloric motor system. J Neurosci 2000;20:6619–6630. [PubMed: 10964967]

Curran-Everett D. Multiple comparisons: philosophies and illustrations. Am J Physiol Regulatory Integrative Comp Physiol 2000;279:R1–R8.

Eisen JS, Marder E. A mechanism for production of phase shifts in a pattern generator. J Neurophysiol 1984;51:1375–1393. [PubMed: 6145759]

Eisen JS, Marder E. Mechanisms underlying pattern generation in lobster stomatogastric ganglion as determined by selective inactivation of identified neurons. III. Synaptic connections of electrically coupled pyloric neurons. J Neurophysiol 1982;48:1392–1415. [PubMed: 6296329]

Golowasch J, Buchholtz F, Epstein IR, Marder E. Contribution of individual ionic currents to activity of a model stomatogastric ganglion neuron. J Neurophysiol 1992;67:341–349. [PubMed: 1373764]

Golowasch J, Marder E. Ionic currents of the lateral pyloric neuron of the stomatogastric ganglion of the crab. J Neurophysiol 1992;67:318–331. [PubMed: 1373762]

Graubard K. Synaptic transmission without action potentials: input-output properties of a nonspiking presynaptic neuron. J Neurophysiol 1978;41:1014–1025. [PubMed: 210264]

Graubard K, Hartline DK. Inactivating outward currents vary among lobster in stomatogastric neurons. Soc Neurosc Abstr. 1984

NIH-PA Author Manuscript

NIH-PA Author Manuscript

NIH-PA Author Manuscript

Graubard K, Hartline DK. Voltage clamp analysis of intact stomatogastric neurons. Brain Res 1991;557:241–254. [PubMed: 1720995]

Graubard K, Raper JA, Hartline DK. Graded synaptic transmission between spiking neurons. Proc Natl Acad Sci U S A 1980;77:3733–3735. [PubMed: 6106194]

Harris-Warrick, RM. Dynamic Biological Networks: The Stomatogastric Nervous System. Harris-Warrick, RM.; Marder, E.; Selverston, AI.; Moulins, M., editors. Cambridge, MA: MIT Press; 1992. p. 87-138.

Harris-Warrick RM. Forskolin reduces a transient potassium current in lobster neurons by a cAMP-independent mechanism. Brain Res 1989;489:59–66. [PubMed: 2545308]

Harris-Warrick RM, Coniglio LM, Barazangi N, Guckenheimer J, Gueron S. Dopamine modulation of transient potassium current evokes phase shifts in a central pattern generator network. J Neurosci 1995a;15:342–358. [PubMed: 7823140]

Harris-Warrick RM, Coniglio LM, Levini RM, Gueron S, Guckenheimer J. Dopamine modulation of two subthreshold currents produces phase shifts in activity of an identified motoneuron. J Neurophysiol 1995b;74:1404–1420. [PubMed: 8989381]

Harris-Warrick RM, Johnson BR, Peck JH, Kloppenburg P, Ayali A, Skarbinski J. Distributed effects of dopamine modulation in the crustacean pyloric network. Ann N Y Acad Sci 1998;860:155–167. [PubMed: 9928309]

Hartline DK, Gassie DV Jr. Pattern generation in the lobster (Panulirus) stomatogastric ganglion. I. Pyloric neuron kinetics and synaptic interactions. Biol Cybern 1979;33:209–222. [PubMed: 497265]

Johnson BR, Harris-Warrick RM. Amine modulation of glutamate responses from pyloric motor neurons in lobster stomatogastric ganglion. J Neurophysiol 1997;78:3210–3221. [PubMed: 9405540]

Johnson BR, Harris-Warrick RM. Aminergic modulation of graded synaptic transmission in the lobster stomatogastric ganglion. J Neurosci 1990;10:2066–2076. [PubMed: 2165519]

Johnson BR, Kloppenburg P, Harris-Warrick RM. Dopamine modulation of calcium currents in pyloric neurons of the lobster stomatogastric ganglion. J Neurophysiol 2003;90:631–643. [PubMed: 12904487]

Johnson BR, Peck JH, Harris-Warrick RM. Amine modulation of electrical coupling in the pyloric network of the lobster stomatogastric ganglion. J Comp Physiol [A] 1993;172:715–732.

Johnson BR, Peck JH, Harris-Warrick RM. Distributed amine modulation of graded chemical transmission in the pyloric network of the lobster stomatogastric ganglion. J Neurophysiol 1995;74:437–452. [PubMed: 7472345]

Kloppenburg P, Levini RM, Harris-Warrick RM. Dopamine modulates two potassium currents and inhibits the intrinsic firing properties of an identified motor neuron in a central pattern generator network. J Neurophysiol 1999;81:29–38. [PubMed: 9914264]

Koshiya N, Smith JC. Neuronal pacemaker for breathing visualized in vitro. Nature 1999;400:360–363. [PubMed: 10432113]

Mamiya A, Manor Y, Nadim F. Short-term dynamics of a mixed chemical and electrical synapse in a rhythmic network. J Neurosci 2003;23:9557–9564. [PubMed: 14573535]

Mamiya A, Nadim F. Dynamic interaction of oscillatory neurons coupled with reciprocally inhibitory synapses acts to stabilize the rhythm period. J Neurosci 2004;24:5140–5150. [PubMed: 15175383]

Mamiya A, Nadim F. Target-specific short-term dynamics are important for the function of synapses in an oscillatory neural network. J Neurophysiol 2005;94:2590–2602. [PubMed: 15972837]

Manor Y, Bose A, Booth V, Nadim F. Contribution of synaptic depression to phase maintenance in a model rhythmic network. J Neurophysiol 2003;90:3513–3528. [PubMed: 12815020]

Manor Y, Nadim F, Abbott LF, Marder E. Temporal dynamics of graded synaptic transmission in the lobster stomatogastric ganglion. J Neurosci 1997;17:5610–5621. [PubMed: 9204942]

Marder E. Polymorphic neural networks. Curr Biol 1994;4:752–754. [PubMed: 7953569]

Marder E, Bucher D. Central pattern generators and the control of rhythmic movements. Curr Biol 2001;11:R986–996. [PubMed: 11728329]

Marder E, Eisen JS. Transmitter identification of pyloric neurons: electrically coupled neurons use different transmitters. J Neurophysiol 1984;51:1345–1361. [PubMed: 6145757]

NIH-PA Author Manuscript

NIH-PA Author Manuscript

NIH-PA Author Manuscript

Marder E, Paupardin-Tritsch D. The pharmacological properties of some crustacean neuronal acetylcholine, gamma-aminobutyric acid, and L-glutamate responses. J Physiol (Lond) 1978;280:213–236. [PubMed: 211227]

Marder E, Thirumalai V. Cellular, synaptic and network effects of neuromodulation. Neural Netw 2002;15:479–493. [PubMed: 12371506]

Maynard DM, Walton KD. Effects of maintained depolarization of presynaptic neurons on inhibitory transmission in lobster neuropil. J Comp Physiol 1975;97:215–243.

Miller JP, Selverston A. Rapid killing of single neurons by irradiation of intracellularly injected dye. Science 1979;206:702–704. [PubMed: 386514]

Miller JP, Selverston AI. Mechanisms underlying pattern generation in lobster stomatogastric ganglion as determined by selective inactivation of identified neurons. IV. Network properties of pyloric system. J Neurophysiol 1982;48:1416–1432. [PubMed: 7153799]

Nadim F, Manor Y. The role of short-term synaptic dynamics in motor control. Curr Opin Neurobiol 2000;10:683–690. [PubMed: 11240276]

Olsen OH, Calabrese RL. Activation of intrinsic and synaptic currents in leech heart interneurons by realistic waveforms. J Neurosci 1996;16:4958–4970. [PubMed: 8756427]

Peck JH, Nakanishi ST, Yaple R, Harris-Warrick RM. Amine modulation of the transient potassium current in identified cells of the lobster stomatogastric ganglion. J Neurophysiol 2001;86:2957–2965. [PubMed: 11731552]

Pena F, Parkis MA, Tryba AK, Ramirez JM. Differential contribution of pacemaker properties to the generation of respiratory rhythms during normoxia and hypoxia. Neuron 2004;43:105–117. [PubMed: 15233921]

Rabbah P, Nadim F. Synaptic dynamics do not determine proper phase of activity in a central pattern generator. J Neurosci 2005;25:11269–11278. [PubMed: 16339022]

Rabbah PM, Atamturktur S, Nadim F. Distinct synaptic dynamics by pacemaker neurons of a rhythmic neural network. Society For Neuroscience. 2002

Ramirez JM, Tryba AK, Pena F. Pacemaker neurons and neuronal networks: an integrative view. Curr Opin Neurobiol 2004;14:665–674. [PubMed: 15582367]

Raper JA. Nonimpulse-mediated synaptic transmission during the generation of a cyclic motor program. Science 1979;205:304–306. [PubMed: 221982]

Rezer E, Moulins M. Expression of the crustacean pyloric pattern generator in the intact animal. J Comp Physiol 1983;153:17–28.

Selverston AI, Russell DF, Miller JP. The stomatogastric nervous system: structure and function of a small neural network. Prog Neurobiol 1976;7:215–290. [PubMed: 11525]

Simmons PJ. Presynaptic depolarization rate controls transmission at an invertebrate synapse. Neuron 2002;35:749–758. [PubMed: 12194873]

Smith JC, Ellenberger HH, Ballanyi K, Richter DW, Feldman JL. Pre-Botzinger complex: a brainstem region that may generate respiratory rhythm in mammals. Science 1991;254:726–729. [PubMed: 1683005]

Thoby-Brisson M, Ramirez JM. Identification of two types of inspiratory pacemaker neurons in the isolated respiratory neural network of mice. J Neurophysiol 2001;86:104–112. [PubMed: 11431492]

Tierney AJ, Harris-Warrick RM. Physiological role of the transient potassium current in the pyloric circuit of the lobster stomatogastric ganglion. J Neurophysiol 1992;67:599–609. [PubMed: 1578246]

Tresch MC, Kiehn O. Motor coordination without action potentials in the mammalian spinal cord. Nat Neurosci 2000;3:593–599. [PubMed: 10816316]

Tryba AK, Ritzmann RE. Multi-joint coordination during walking and foothold searching in the Blaberus cockroach. II. Extensor motor neuron pattern. J Neurophysiol 2000;83:3337–3350. [PubMed: 10848553]

Turrigiano, GG.; Heinzel, HG. Behavioral correlates of stomatogastric network function. In: Harris-Warrick, RM.; Marder, E.; Selverston, AI.; Moulins, M., editors. Dynamic Biological Networks: The Stomatogastric Nervous System. Cambridge, MA: MIT Press; 1992. p. 197-220.

Wallen P, Grillner S. N-methyl-D-aspartate receptor-induced, inherent oscillatory activity in neurons active during fictive locomotion in the lamprey. J Neurosci 1987;7:2745–2755. [PubMed: 3040925]

Wolf H. Reflex modulation in locusts walking on a treadwheel-intracellular recordings from motoneurons. J Comp Physiol 1992;170:443–462.

NIH-PA Author Manuscript

NIH-PA Author Manuscript

NIH-PA Author Manuscript

NIH-PA Author Manuscript

NIH-PA Author Manuscript

NIH-PA Author Manuscript

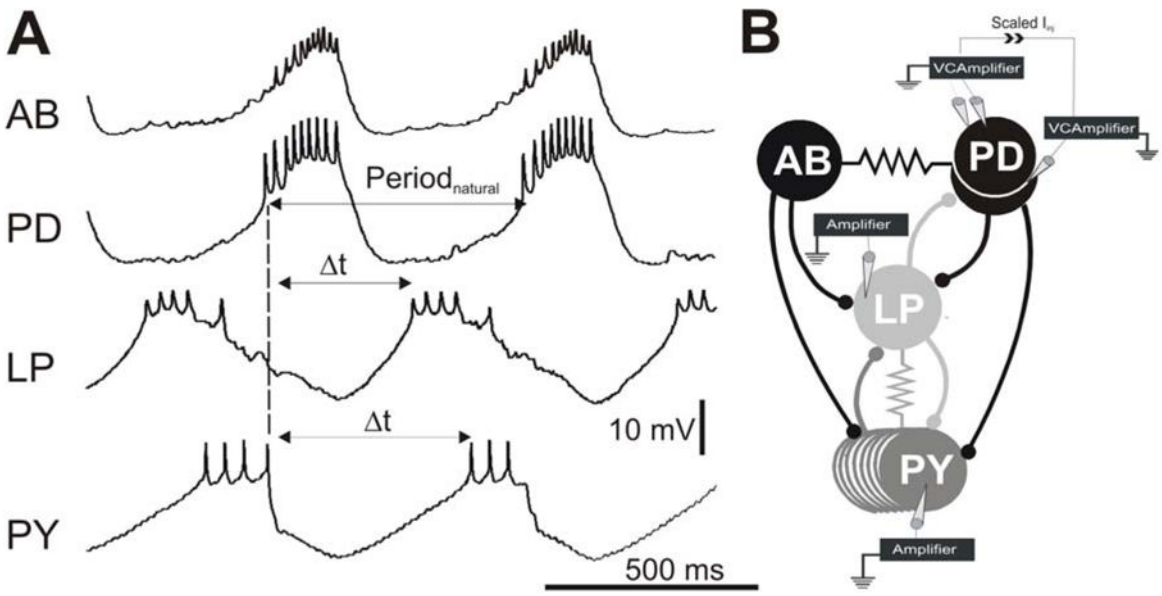

Figure 1. The pyloric network and experimental protocol

A. Simultaneous intracellular recordings indicate that the AB and PD neurons oscillate in synchrony and inhibit the follower LP and PY neurons which burst out of phase with the AB/PD neurons and each other. The PD burst onset was used a reference point (dashed line) to calculate $Period_{natural}$ and the LP and PY burst phases. Phase is calculated by dividing the time difference between burst onsets (t) by $Period_{natural}$. The baselines for the membrane potential oscillations were −62 mV for AB, −57 mV for PD, −58 mV for LP and −62 mV for PY. For simplicity, recording of only one of two PD neurons is shown. **B.** The synaptic connectivity and the experimental paradigm represented schematically. All chemical synaptic connections (ball and stick symbols) are inhibitory; resistor symbols indicate gap-junctional couplings. All neurons were impaled with one electrode except for one PD neuron which was impaled with two for voltage clamp. The current used to voltage clamp that PD neuron was scaled and injected into the other PD neuron to voltage clamp the latter neuron to the same V_{clamp} value. Paired recordings of the LP and PY neurons were carried out in current clamp.

NIH-PA Author Manuscript

NIH-PA Author Manuscript

NIH-PA Author Manuscript

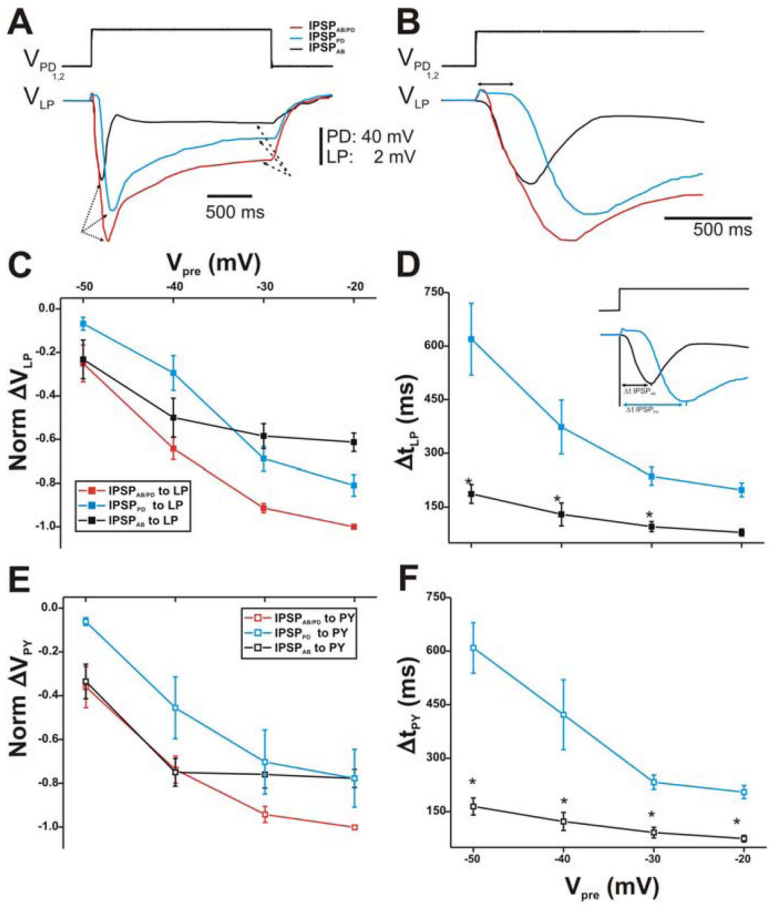

Figure 2. Postsynaptic potentials of the LP and PY neurons in response to stimulations of the PD neurons with a single square pulse

A. The membrane potentials of the PD neurons were stepped from −60 mV to −20 mV (top trace). The red trace represents combined IPSPs from both the AB and PD neurons ($IPSP_{AB/PD}$; red trace) in control (TTX saline). In PTX, the AB synaptic output is blocked and the response in the LP neuron is due to the synapse from the PD neurons only ($IPSP_{PD}$; blue trace). The $IPSP_{PD}$ trace was subtracted from $IPSP_{AB/PD}$ to yield the synapse due to the AB neuron only ($IPSP_{AB}$; black trace). All IPSPs exhibited a transient peak (dotted arrows) that decayed to a sustained value (dashed arrows). The LP neuron had an initial membrane potential of−59 mV. **B**. A close-up of the IPSPs in A shows that the time courses of the synaptic response in all conditions were different from each other. The double headed arrow represents the delay in onset of the synaptic response of the PD neurons. **C.** Synaptic I/O curve for square pulses of 10–40 mV amplitudes used to depolarize the presynaptic PD neurons (N = 6). The values were normalized to the amplitude $IPSP_{AB/PD}$ in response to a step to −20 mV. The amplitude of each IPSP is measured from V_{rest} to the maximal value of the IPSP. The results show that for V_{pre} of −50 and −40 mV (from −60 mV), the compound synapse to the LP neuron was mostly from the AB neuron. $IPSP_{PD}$ required more positive PD potentials to activate compared to both $IPSP_{AB/PD}$ and $IPSP_{AB}$ onto LP. **D.** The time to peak of the IPSPs was measured from the beginning of the presynaptic depolarization to the maximal peak of the IPSP (inset). $IPSP_{PD}$ onto the LP neuron reached its maximum peak value slower than $IPSP_{AB}$. Moreover, both IPSPs showed a dependence on the presynaptic potential (N = 6). **E.** Same as in panel C, but using the PY neuron as the postsynaptic target. The response is similar to that seen in the

LP neuron. **F.** Same as in panel D, but using the PY neuron as the postsynaptic target. Again, the results were similar to those of the LP neuron. (* indicates significant difference).

NIH-PA Author Manuscript
NIH-PA Author Manuscript
NIH-PA Author Manuscript

NIH-PA Author Manuscript

NIH-PA Author Manuscript

NIH-PA Author Manuscript

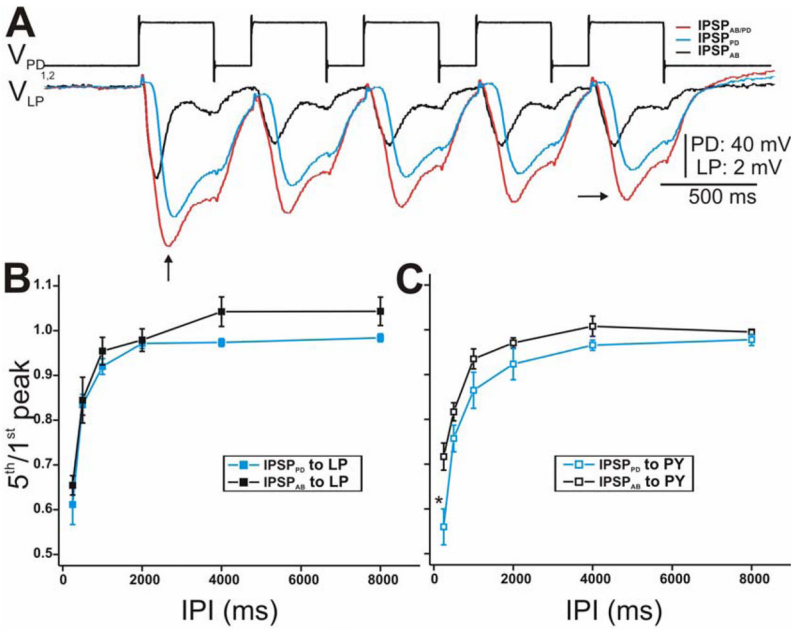

Figure 3.

Synaptic dynamics of the IPSPs in response to a train of voltage pulses in the PD neurons. **A.** The PD neurons were stimulated with a series of 5 pulses of 40 mV amplitude from V_{hold} = −60 mV with IPI 250 ms in control (red) and PTX (blue) while the response in the LP neuron was monitored. $IPSP_{AB}$ was approximated by subtracting the two traces (black trace). All IPSPs in response to the 5^{th} pulse (horizontal arrow) were smaller in amplitude than the 1^{st} pulse IPSPs (vertical arrow) indicating short-term synaptic depression. Note that we measure the amplitude of each IPSP from V_{rest} of the LP neuron. The LP neuron had an initial membrane potential of −59 mV. **B.** The extent of depression of the LP IPSP response was calculated as the ratio of the 5^{th} peak amplitude to the amplitude of the 1^{st} peak for all IPIs used (250–8000 ms). The data was plotted vs IPI (N = 6). The extent of depression of $IPSP_{PD}$ was similar to that of $IPSP_{AB}$ at all IPIs **C.** Same as in B using PY as the postsynaptic neuron. (* indiates significant difference).

NIH-PA Author Manuscript

NIH-PA Author Manuscript

NIH-PA Author Manuscript

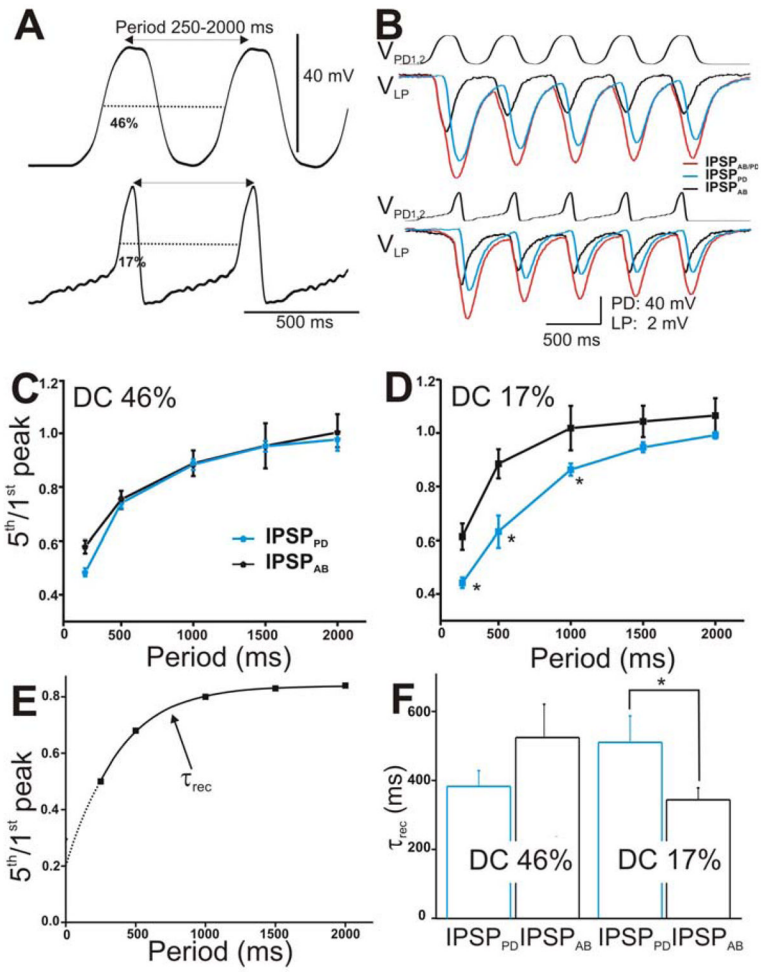

Figure 4. The IPSPs in the LP neuron in response to a train of two realistic PD waveforms

A. The PD neurons were stimulated with two types of realistic waveforms, DC 46% (top trace) and DC 17% (bottom panel). Both waveforms were pre-recorded in the PD neuron from two different preps, low-pass filtered (at 10 Hz) and amplified to 40 mV amplitudes. They were injected from Vh = −60 mV in a train of 5 pulses with frequencies ranging from 0.5–4 Hz. **B.** The LP response to DC 46% (top panel) and DC 17% (bottom panel) with cycle period 500 ms. The IPSPs elicited by the individual AB (black trace) and PD neurons (blue trace) and by the compound AB/PD unit (red trace) are superimposed for comparison. **C.** Extent of depression of the IPSPs ($5^{th}/1^{st}$ peak) in response to DC 46% was plotted vs. cycle periods (N = 6). **D.** Extent of depression of the IPSPs in response to DC 17% plotted vs. cycle periods showed that $IPSP_{AB}$ exhibited significantly less depression (marked by *) than $IPSP_{PD}$ for cycle periods 250–1000 ms (N = 6). **E.** The time constant of recovery from depression of the IPSPs was calculated by fitting the $5^{th}/1^{st}$ ratio vs. cycle periods for each experiment with a single exponential fit (dashed line). **F.** Average τ_{rec} values showed that for DC 17%. $IPSP_{AB}$ recovered significantly faster than $IPSP_{PD}$ (N = 6). (* indicates significant difference).

NIH-PA Author Manuscript

NIH-PA Author Manuscript

NIH-PA Author Manuscript

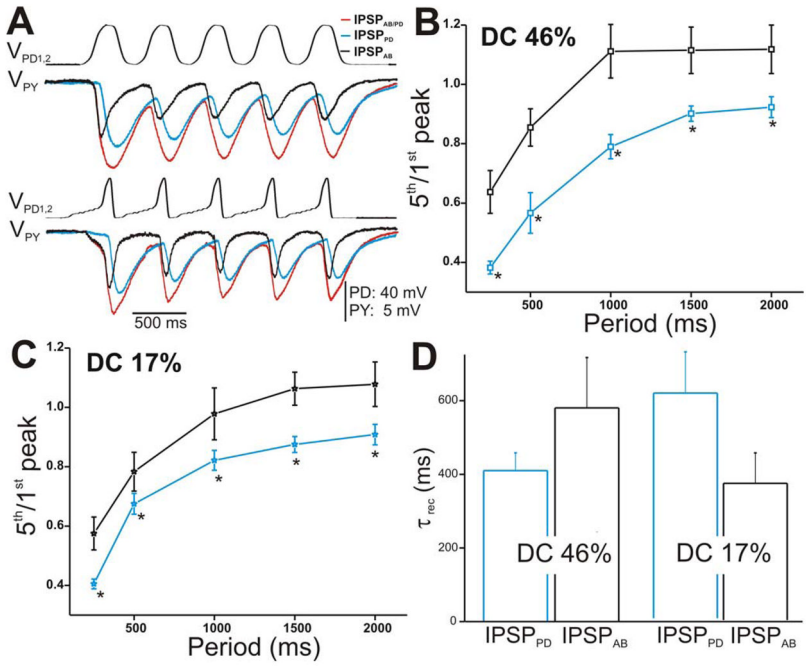

Figure 5. The IPSPs in the PY neuron in response to a train of two realistic PD waveforms

A. The PY response to the stimulation of the PD neurons with DC 46% (top panel) and DC 17% (bottom panel) corresponding to amplitude 40 mV and cycle period 500 ms. **B.** Ratio $5^{th}/1^{st}$ peak in response to DC 46% plotted vs. cycle periods showed that $IPSP_{AB}$ depressed significantly less than $IPSP_{PD}$ (N = 6). Again, the amplitudes of the IPSPs were measured from V_{rest}. **C.** Similar to B, the extent of depression of $IPSP_{AB}$ in response to DC 17% was significantly less than $IPSP_{PD}$. **D.** Average τ_{rec} values of the IPSPs calculated as in Figure 4E (N = 6). (* indicates significant difference).

NIH-PA Author Manuscript

NIH-PA Author Manuscript

NIH-PA Author Manuscript

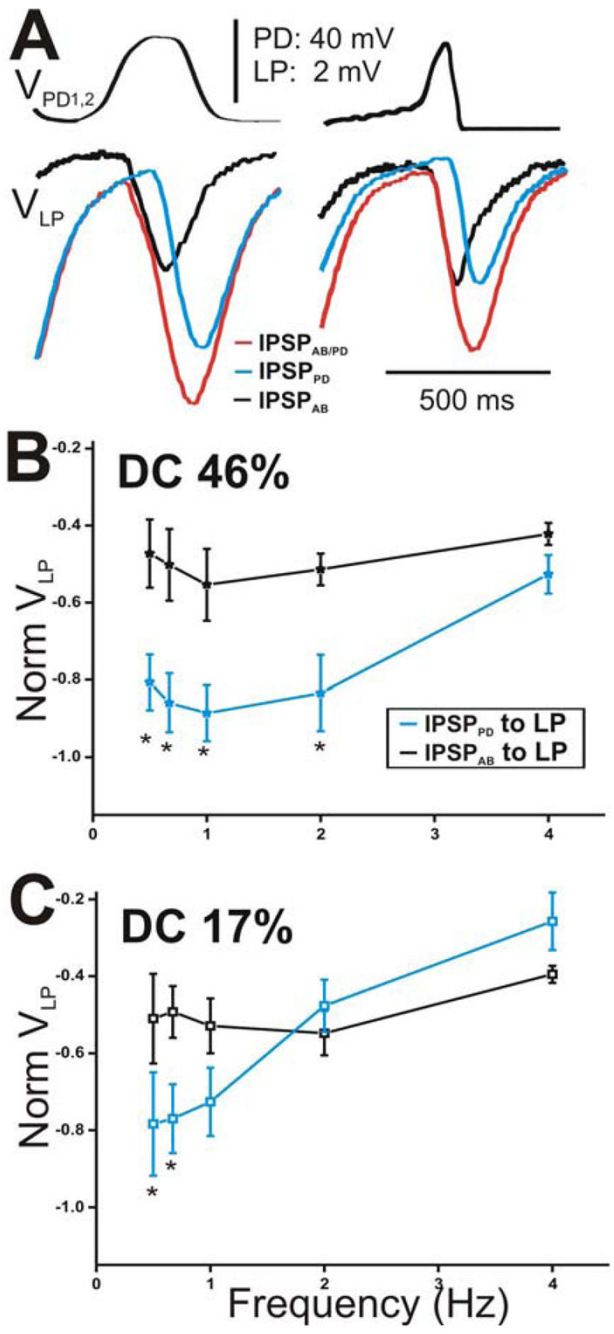

Figure 6.

The peak amplitude of the IPSPs in the LP neuron appeared sensitive to the slope of the rising phase of the presynaptic depolarizations. **A.** The IPSPs in response to the 5th waveform (see Fig. 5A) elicited with DC 46% (left panel) and 17% (right panel) corresponding to cycle period 500 ms. The amplitude of $IPSP_{AB}$ is smaller than that of $IPSP_{PD}$ for DC 46% only. **B.** The steady-state amplitudes of $IPSP_{PD}$ and $IPSP_{AB}$ were normalized to the steady-state amplitudes of $IPSP_{AB/PD}$ at frequency 0.67 Hz for DC 46%. The values were plotted as a function of presynaptic frequency. The relative contribution of $IPSP_{PD}$ was significantly larger for the lowest frequencies (N = 6). **C.** The amplitudes of the IPSPs in response to DC 17% were

normalized as in B and plotted vs. frequency (N = 6). Results obtained were similar to those in B. (* indicates significant difference).

NIH-PA Author Manuscript
NIH-PA Author Manuscript
NIH-PA Author Manuscript

NIH-PA Author Manuscript

NIH-PA Author Manuscript

NIH-PA Author Manuscript

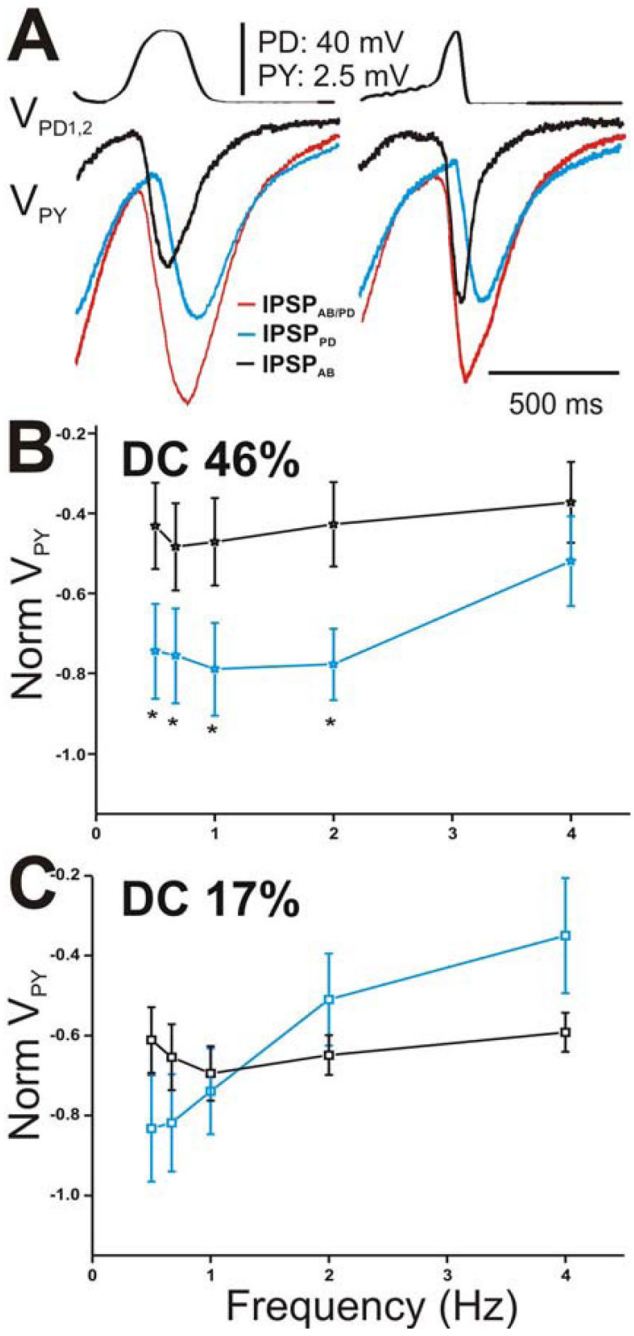

Figure 7.

The peak amplitude of the IPSPs in the PY neuron appeared sensitive to the slope of the rising phase of the presynaptic depolarizations. **A.** The IPSPs in response to the 5th waveform elicited with DC 46% (left panel) and 17% (right panel) corresponding to cycle period 500 ms. $IPSP_{AB}$ is smaller in amplitude than $IPSP_{PD}$ for DC 46% and equal in amplitude for DC 17%. **B.** The steady-state amplitudes of $IPSP_{PD}$ and $IPSP_{AB}$ in the PY neurons were normalized and plotted as a function of presynaptic frequency as in Figure 6. The relative contributions of both the AB and PD components were not significantly different from each other at all frequencies tested (N = 6). **C.** The amplitudes of the IPSPs in response to DC 17% were normalized as in

NIH-PA Author Manuscript

NIH-PA Author Manuscript

NIH-PA Author Manuscript

Figure 6 and plotted vs. frequency. Again, no significant difference between the amplitudes at all frequencies tested (N = 6). (* indicates significant difference).

NIH-PA Author Manuscript

NIH-PA Author Manuscript

NIH-PA Author Manuscript

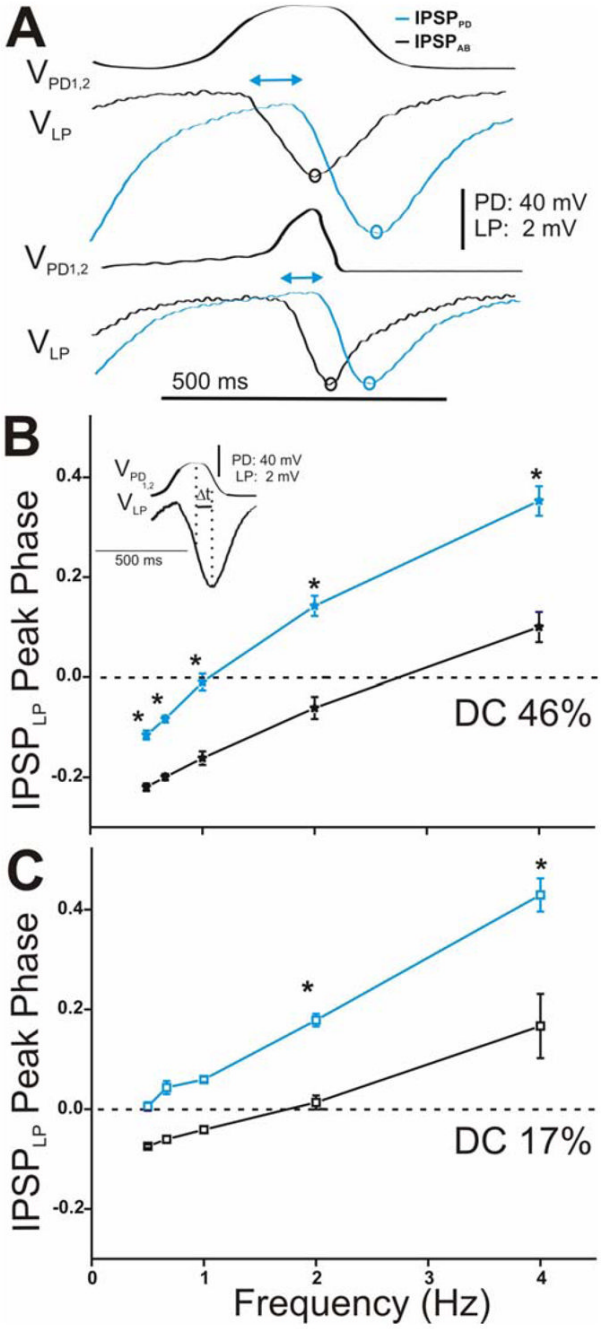

Figure 8.

Time course of synaptic transmission of the IPSPs in the LP neuron in response to the realistic waveform stimulations in the PD neurons and its effect on the LP IPSP peak phase. **A.** The IPSPs in response to the 5th waveform elicited with DC 46% (top panel) and 17% (bottom panel) at cycle frequency 2 Hz showed that $IPSP_{PD}$ (blue open circles) reached its maximum peak significantly later in time than $IPSP_{AB}$ (black open circles) independent of the duty cycle of the waveform used. The double headed arrows are only meant to represent the delay between the start of hyperpolatization in the LP neuron due to the AB vs. the PD synapse. **B.** LP IPSP peak phase was calculated as t (measured form the peak of the presynaptic waveform to the peak IPSP) divided by $Period_{applied}$ (inset) and plotted vs. frequency (N = 6). In response to

DC 46%, the LP IPSP peak phase was significantly delayed due to the synapse from the PD neurons (blue trace). **C.** Similar results were obtained for DC 17% (N = 6). (* indicates significant difference).

NIH-PA Author Manuscript
NIH-PA Author Manuscript
NIH-PA Author Manuscript

NIH-PA Author Manuscript

NIH-PA Author Manuscript

NIH-PA Author Manuscript

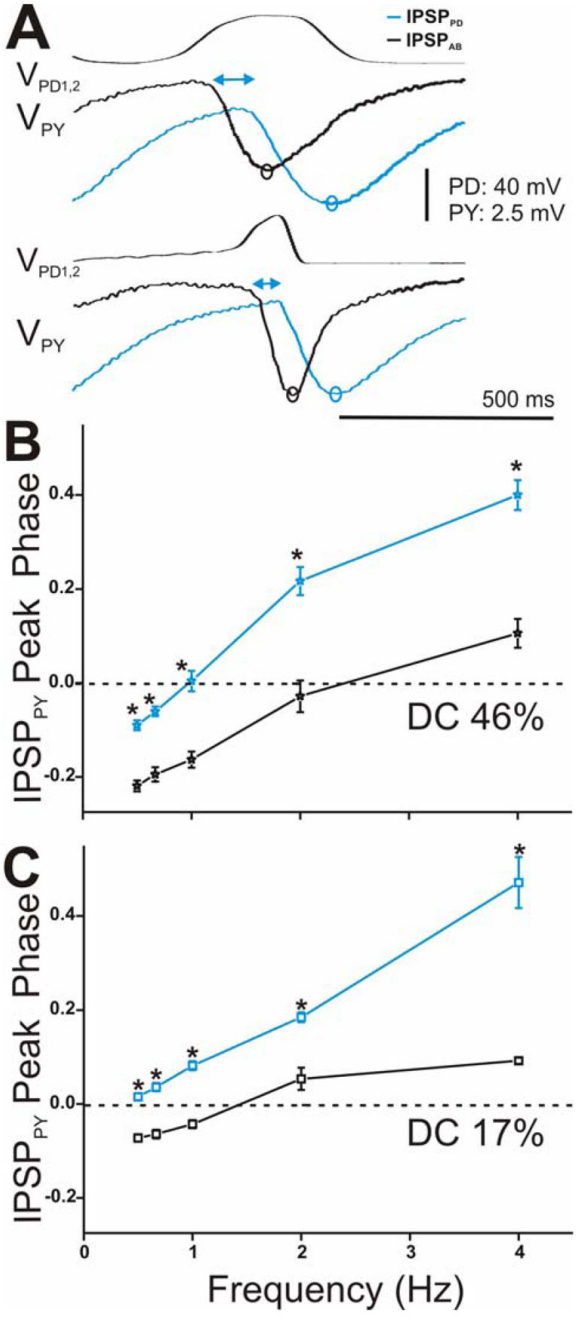

Figure 9.

Time course of synaptic transmission of the IPSPs in the PY neuron in response to the realistic waveform stimulations and its effect on the PY phase. **A.** The IPSPs in response to the 5th waveform elicited with DC 46% (top panel) and 17% (bottom panel) at cycle frequency 2 Hz showed that $IPSP_{PD}$ (blue open circles) reached its maximum peak significantly later in time than $IPSP_{AB}$ (black open circles) independent of the duty cycle of the waveform used. The double headed arrows are only meant to represent the delay between the start of hyperpolatization in the PY neuron due to the AB vs. the PD synapse. **B. and C.** PY IPSP peak phase was calculated as in Figure 8B and plotted vs. frequency (N = 6). Results were similar

to those reported for the LP neuron for both DC 46% (**B**, N = 6) and DC 17% (**C**, N = 6). (* indicates significant difference).

NIH-PA Author Manuscript
NIH-PA Author Manuscript
NIH-PA Author Manuscript

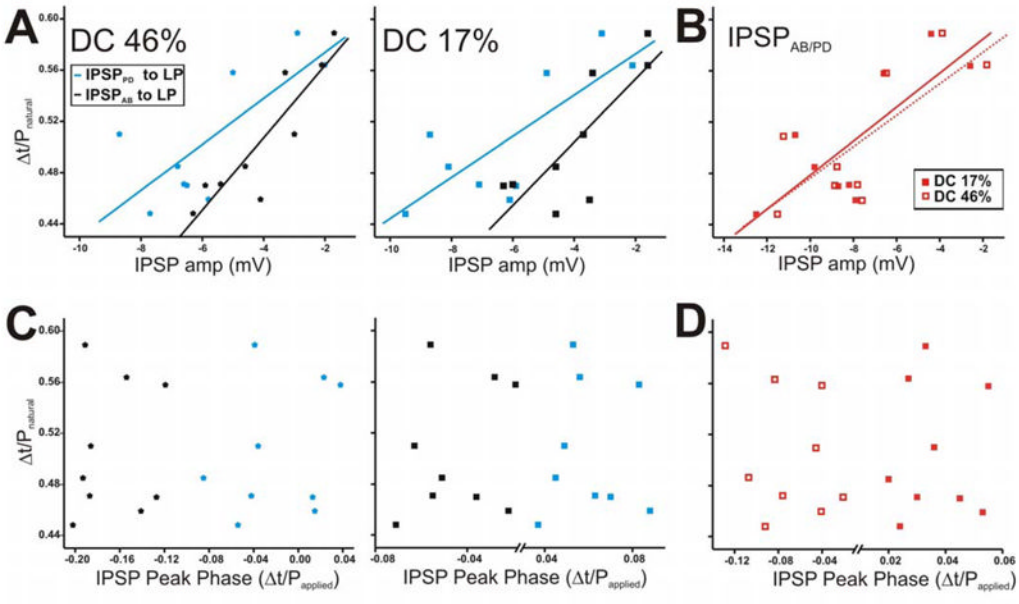

Figure 10.

The LP burst phase in the ongoing rhythm is positively correlated with the amplitude of the AB and PD synapses but not with their peak phase. The LP burst phase in the ongoing rhythm was measured using the natural pyloric period and the PD neuron as a reference point. The IPSP values chosen for this figure are those corresponding to cycle $period_{applied}$ of 1 s. Each point in the graph represents one preparation. **A.** The LP burst phase during the ongoing rhythm showed a strong positive correlation to the IPSP amplitudes due to AB and PD neurons, for both DC 46% (left panel) and 17% (right panel). **B.** The LP burst phase plotted vs. the IPSP amplitudes due to the AB/PD unit for DC 46% and 17%. **C.** The IPSP peak phase was calculated using the time to peak with respect to the peak of the presynaptic waveform (see Fig. 8B inset for example) and plotted vs. the LP burst phase during the ongoing rhythm for DC 46% (left panel) and 17% (right panel). **D.** Scatter plot of $IPSP_{AB/PD}$ peak phase in DC 46% vs. 17% showed no correlation to the LP burst phase. Solid diagonal lines in A and B are best linear fits.

NIH-PA Author Manuscript NIH-PA Author Manuscript NIH-PA Author Manuscript

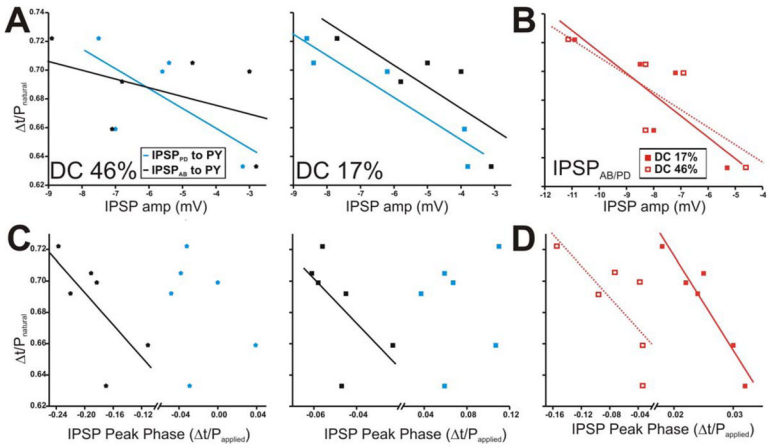

Figure 11.

The PY burst phase in the ongoing rhythm is negatively correlated with some dynamic parameters of the AB and PD synapses. The PY burst phase in the ongoing rhythm is calculated as in Fig. 10. **A.** The PY burst phase during the ongoing rhythm tended to be negatively correlated to the amplitudes of $IPSP_{AB}$ and $IPSP_{PD}$ for DC 17% only (right panel). **B.** The amplitudes of $IPSP_{AB/PD}$ for DC 46% and 17% also tended to be negatively correlated to the PY burst phase. **C.** The IPSP peak phase was calculated as in Fig. 10 and plotted vs. the PY burst phase during the ongoing rhythm for DC 46% (left panel) and 17% (right panel). **D.** Correlation of $IPSP_{AB/PD}$ peak phase in DC 46% vs. 17% to the PY burst phase. Solid diagonal lines in all panels are best linear fits.

NIH-PA Author Manuscript NIH-PA Author Manuscript NIH-PA Author Manuscript